Development • Advance article

Regulatory logic driving stable levels of *defective proventriculus* expression during terminal photoreceptor specification in flies

Jenny Yan[1,3], Caitlin Anderson[1], Kayla Viets[1], Sang Tran[1], Gregory Goldberg[2, 4], Stephen Small[2], and Robert J. Johnston Jr.[1, #]

1. Department of Biology, Johns Hopkins University, 3400 N. Charles Street
Baltimore, MD 21218-2685, USA

2. Center for Developmental Genetics, Department of Biology, New York University,
100 Washington Square East, New York, NY 10003-6688, USA

3. Current address: Department of Genetics, Harvard Medical School, 77 Avenue Louis
Pasteur, Boston, MA 02115, USA

4. Current address: Laboratory of Bacteriology, The Rockefeller University, New York,
New York 10065, USA

Corresponding Author. email: robertjohnston@jhu.edu

Abstract

How differential levels of gene expression are controlled in post-mitotic neurons is poorly understood. In the *Drosophila* retina, expression of the transcription factor Defective Proventriculus (Dve) at distinct cell-type-specific levels is required for terminal differentiation of color- and motion-detecting photoreceptors. Here, we find that the activities of two *cis*-regulatory enhancers are coordinated to drive *dve* expression in the fly eye. Three transcription factors act on these enhancers to determine cell-type-specificity. Negative autoregulation by Dve maintains expression from each enhancer at distinct homeostatic levels. One enhancer acts as an inducible backup ("dark" shadow enhancer) that is normally repressed but becomes active in the absence of the other enhancer. Thus, two enhancers integrate combinatorial transcription factor input, feedback, and redundancy to generate cell-type specific levels of *dve* expression and stable photoreceptor fate. This regulatory logic may represent a general paradigm for how precise levels of gene expression are established and maintained in post-mitotic neurons.

Keywords

expression levels, gene regulation, post-mitotic neurons, photoreceptor, fly eye, *Drosophila*, retina, R7, R8, outer photoreceptors*, Rhodopsin3, Rhodopsin4, Rhodopsin5, Rhodopsin6, defective proventriculus, spineless, orthodenticle, spalt,* negative feedback, shadow enhancer, dark shadow enhancer, robustness

Introduction

Genes are expressed at distinct cell-type-specific levels at different times during development. Expression is often transient, arising for short periods of time to trigger downstream regulatory pathways. For example, expression driven by the *eve* stripe 2 enhancer, perhaps the best-understood regulatory DNA element, is very short-lived, persisting for only ~15 minutes after the mature stripe is fully formed during embryonic development in flies (Bothma et al., 2014). In contrast, gene expression in post-mitotic neurons must be maintained on long timescales, often for the lifetime of the organism. Establishing and maintaining distinct levels of transcription factors is particularly important for neuronal fate and function across species. For example, in worms, low levels of the transcription factor MEC-3 specify the elaborate dendritic patterning of PVD pain-sensing neurons, while high MEC-3 determines the simple morphology of AVM and PVM touch neurons (Smith et al., 2013). Similarly, flies use differences in levels of the homeodomain transcription factor Cut to control dendritic branching complexity in sensory neuron subtypes (Grueber et al., 2003). In mice, the Hox accessory factor FoxP1 acts as a dose-dependent determinant of motor neuron subtype identity (Dasen et al., 2008). Beyond these cases, there are numerous examples of differential transcription factor expression in neuronal subtypes whose roles are not understood, such as the differential expression of Brn3b in ipRGC subtypes (Chen et al., 2011).

Establishing and maintaining distinct levels of gene expression for the lifetime of a neuron presents specific challenges. Regulatory mechanisms must ensure that expression levels remain in a narrow range for days and even years while providing robustness against acute perturbations caused by activity and environment. In some cases, the transcription factors that dictate cell-type-specific expression levels have been identified (Corty et al., 2016), but how these regulatory inputs are interpreted by DNA elements has not been characterized. Further, it is unclear how transcription factor feedback and *cis*-regulatory redundancy contribute to ensuring proper expression levels in neurons.

Expression of transcription factors at cell-type-specific levels is required for the terminal specification of motion- and color-detecting photoreceptors in the *Drosophila* retina. The *Drosophila* compound eye consists of approximately 800 ommatidia, or unit eyes, each containing eight photoreceptors (PRs) (Wolff, 1993) (**Fig. 1E**). The outer PRs (R1-R6) express the broad spectrum-sensitive Rhodopsin 1 (Rh1) and detect motion (Hardie, 1985), whereas the inner PRs (R7 and R8) express color-sensitive Rhodopsin proteins (Rh3-Rh6) (Gao et al., 2008; Yamaguchi et al., 2010). Two ommatidial subtypes, pale (**p**) and yellow (**y**), are randomly distributed in the retina at a ratio of 35:65 (Bell et al., 2007; Franceschini et al., 1981)(**Fig. 1B-D**). The **p** subtype contains UV-sensitive Rh3 in **p**R7 and blue-sensitive Rh5 in **p**R8, whereas the **y** subtype contains UV-sensitive Rh4 in **y**R7 and green-sensitive Rh6 in **y**R8 (**Fig. 1A-C**) (Chou et al., 1996; Fortini and Rubin, 1990; Johnston and Desplan, 2010). The specification of these photoreceptor subtypes is controlled by a complex network of transcription factors and other regulators (Hsiao et al., 2013; Jukam and Desplan, 2011; Jukam et al., 2016; Jukam et al., 2013; Mikeladze-Dvali et al., 2005; Viets et al., 2016; Wernet et al., 2006).

Differential expression of the K50 homeodomain transcription factor Defective proventriculus (Dve) is critical for terminal specification of photoreceptors in the fly eye

(Johnston et al., 2011; Thanawala et al., 2013). Dve is expressed in a unique pattern, with high levels in the outer PRs, low levels in **y**R7s, and no expression in **p**R7s or R8s (**Fig. 1K**). High Dve in motion-detecting outer PRs represses expression of color-detecting Rh3, Rh5, and Rh6. Low levels of Dve in **y**R7s repress Rh3 to maintain exclusive expression of Rh4 in **y**R7 subtypes in the main ventral region of the retina (**Fig. 1L, N**). In the dorsal third, Dve levels are lowered further in **y**R7s to allow co-expression of Rh3 in Rh4-expressing cells (**Fig. 1D**). The absence of Dve expression allows expression of Rh3 in **p**R7s (**Fig. 1M-N)** and Rh5 and Rh6 in R8s (Johnston et al., 2011).

Changes in levels of Dve expression have a dramatic impact on Rhodopsin expression and photoreceptor fate. In *dve* null mutants, Rh3 is derepressed in all R7s and Rh3, Rh5 and Rh6 are variably expressed in outer PRs (**Fig. 1O-Q**) (Johnston et al., 2011; Sood et al., 2012). In *dve* hypomorphic mutants, where levels of Dve are lowered but not completely lost, Rh3 is still derepressed in all R7s, but only Rh6 is expressed in outer PRs (Johnston et al., 2011). When Dve levels are subtly lowered upon mutation of upstream regulators, the dorsal region of Rh3 and Rh4 co-expression is expanded from one third of the retina to the entire dorsal half (Thanawala et al., 2013). The misexpression of Rhs in *dve* mutants causes defects in low-intensity light discrimination (Johnston et al., 2011). Deleterious effects are also seen when Dve levels are increased: raising levels of Dve in **y**R7s causes loss of Rh3/Rh4 co-expression in the specialized dorsal third region (Mazzoni et al., 2008; Thanawala et al., 2013), whereas overexpression in R8s represses Rh5 and Rh6 completely (Johnston et al., 2011). Thus, the differential expression of *dve* in photoreceptors is important for proper Rh expression and visual function.

Cell-type-specific levels of Dve are achieved through regulation by the K50 homeodomain transcription factor Orthodenticle (Otd), the zinc-finger transcription factors Spalt major and Spalt related (referred to collectively as Spalt (Sal)), and the PAS-bHLH transcription factor Spineless (Ss). Otd activates Dve in all PRs (**Fig. 1F**), Sal represses Dve in the inner PRs (**Fig. 1G-H)**, and Ss re-activates Dve in **y**R7s (**Fig. 1I-J**)(Johnston, 2013; Johnston et al., 2011).

To determine how these transcription factors dictate cell-type-specific levels of Dve expression, we analyzed the *cis*-regulatory logic controlling *dve* and identified two enhancers, ***y****R7 enh* and *outer enh,* which together induced expression recapitulating endogenous Dve expression. ***y****R7 enh* is activated by Ss, Sal, and Otd in **y**R7 cells while *outer enh* is activated by Otd in all PRs and repressed by Sal in inner PRs. Negative feedback by Dve onto both enhancers maintains proper levels of Dve expression. This autoregulation is particularly important for ***y****R7 enh,* which is dramatically upregulated in **y**R7s when Dve feedback is ablated. Interestingly, we also observed de-repression of ***y****R7 enh* in outer PRs in *dve* mutants, suggesting that ***y****R7 enh* serves as an inducible backup or "dark" shadow enhancer in these cells. Shadow enhancers are DNA elements that drive redundant expression patterns and ensure robust gene expression in cases of genetic and environmental perturbation (Bothma et al., 2015; Frankel et al., 2010; Hong et al., 2008; Miller et al., 2014; Nolte et al., 2013; Perry et al., 2010; Wunderlich et al., 2015). ***y****R7 enh* represents an unusual "dark" shadow enhancer since it is normally repressed and only becomes active when Dve driven by the primary *outer enh* is compromised. Together, the ***y****R7 enh* and *outer enh* integrate combinatorial transcription factor input, negative feedback, and redundancy to ensure distinct cell-type-specific levels of *dve* expression required for stable photoreceptor specification.

Results

Two enhancers determine yR7- and outer PR-specific expression of Dve

The *dve* gene locus is ~65 kb with two alternative transcriptional starts driven by the *dve-A* promoter or *dve-B* promoter (**Fig. 2A**). Deletion of the *dve-A* promoter caused de-repression of Rh3 in **y**R7s in the dorsal half of the retina (**Fig. S1A-B**), while Rh5 and Rh6 expression were unaffected (**Fig. S1C**). This incomplete *dve* phenotype is consistent with a decrease in Dve levels in **y**R7s (Thanawala et al., 2013), suggesting that the *dve-A* promoter is required for normal Dve expression. To test the role of the *dve-B* promoter, we employed a CRISPR strategy to delete a ~1.5 kb region encompassing the *dve-B* promoter and first exon. Deletion of the *dve-B* promoter did not alter Dve-regulated Rh expression (**Fig. S1D-F**), suggesting that the *dve-B* promoter is not required for Dve expression. Since the *dve-A* promoter is required for normal Dve expression, we used this promoter as the minimal promoter in enhancer reporters.

To identify *cis*-regulatory elements controlling *dve* expression, we generated transgenes containing 3-6 kb DNA fragments from the *dve* locus and the *dve-A* promoter driving nuclear GFP (**Fig. 2A,** *dve enh>GFP*). The *dve-A* promoter alone drove extremely weak GFP expression in pigment cells and R4 PRs, and therefore did not recapitulate normal Dve expression in all outer PRs and **y**R7s (**Fig. S1H**).

Two constructs drove GFP expression that together recapitulated endogenous Dve expression in midpupation (i.e. ~48 APF). *outer enh* drove expression in outer PRs (**Fig. 2A, E**), and ***y**R7 enh* drove expression specifically in a subset of R7s (**Fig. 2A-B**). This subset corresponded to **y**R7 fate, since 68% of R7s had strong GFP expression and perfectly co-expressed Ss (i.e. **y**R7s), while 32% had weak or no GFP and lacked Ss (i.e. **p**R7s)(**Fig. 2B-D).**

Additionally, *weak **y**R7 enh* drove weak expression in **y**R7s (**Fig. 2A, S1M-O,** described further below), and *dorsal R7 enh* drove expression in dorsal posterior R7s, (**Fig. 2A, S1P-Q**). Four enhancers drove weak expression in all PRs (*all PRs enh 1-4)* (**Fig. 2A, S1I-L**).

Janelia Research Campus and the Vienna Drosophila Resource Center (VDRC) both generated lines that express GAL4 driven by fragments of the *dve* locus (**Fig. 2A**). Expression driven by these fragments was consistent with results from our *dve enh* reporter constructs. GMR40E08, a ~3kb fragment that overlaps with *outer enh*, drove strong GFP expression in outer PRs, while other constructs that either did not overlap or only partially overlapped with *outer enh* or ***y**R7 enh* did not show significant expression (**Fig. 2A**).

Since ***y**R7 enh* and *outer enh* recapitulated endogenous Dve expression, we further characterized the temporal dynamics of these two enhancers. At midpupation, Dve protein is expressed strongly in outer PRs and weakly in **y**R7s (Johnston et al., 2011), similar to GFP expression driven by ***y**R7 enh* and *outer enh* (**Fig. S2B, F, J**). In 3rd instar larvae, analysis of Dve protein expression was obscured by non-specific antibody staining (**Fig. S2A**) (Johnston et al., 2011). While *outer enh* was not expressed, ***y**R7 enh* was expressed in a subset of R7s (**Fig. S2E, I**), suggesting that Dve is expressed in larval **y**R7s. In adults, Dve protein is expressed in **y**R7s and outer PRs (**Fig. S2C-D**). Similarly, *outer enh* drove GFP expression in outer PRs in adults (**Fig. S2K-L**). ***y**R7 enh* drove expression in all R7s in adults (**Fig. S2G-H**), suggesting that additional activators present only in the adult stage induce ***y**R7 enh* expression in all R7s, and that this enhancer is missing DNA elements that prevent ectopic Dve expression in adults.

Together, the spatiotemporal dynamics of these enhancers are consistent with endogenous *dve* expression. Next, we tested how upstream transcription factors control expression of these two enhancers.

yR7 enh is activated by Ss, Sal, and Otd

***y**R7 enh* drives expression in **y**R7 cells (**Fig. 3A**). Dve is expressed at lower levels in **y**R7s in the dorsal third, allowing IroC-induced activation of Rh3 and co-expression of Rh3 and Rh4 (Johnston et al., 2011). Similar to endogenous Dve expression, ***y**R7 enh* is expressed at lower levels in dorsal third (DT) **y**R7s as compared to the rest of the retina (**Fig. 3D**).

Otd is required for Dve expression in **y**R7s (Johnston et al., 2011). ***y**R7 enh* failed to induce expression in **y**R7s in *otd* mutants, suggesting that Otd is required for activation of this enhancer (**Fig. 3B**).

Ss induces expression of Dve in **y**R7s (Johnston et al., 2011). Expression of ***y**R7 enh* was lost in *ss* mutants (**Fig. 3C**). Ectopic expression of Ss in all PRs induced strong

***y**R7 enh* expression in all R7s and weak expression in all other PRs (**Fig. 3E**), suggesting that another factor acts with Ss to activate strong ***y**R7 enh* expression.

Since Sal is important for R7 fate (Mollereau et al., 2001), we posited that Sal may work with Ss to activate ***y**R7 enh*. Expression of ***y**R7 enh* was completely lost in *sal* mutants (**Fig. 3F**), while ectopic expression of Sal in all PRs induced ***y**R7 enh* expression in a random subset of R1 and R6 outer PRs (**Fig. 3G)**. We showed previously that ectopic Sal induced Ss in a random subset of R1 and R6 outer PRs (Johnston and Desplan, 2014). These data suggest that Ss and Sal function together to activate expression of ***y**R7 enh*.

Supporting our hypothesis, ectopic expression of both Ss and Sal induced strong ***y**R7 enh* expression in all PRs (**Fig. 3H**), suggesting that Ss and Sal both activate expression of ***y**R7 enh*. Since Sal induces expression of Ss, and Ss together with Sal induces ***y**R7 enh*, Ss, Sal, and ***y**R7 enh* form a coherent feedforward loop (**Fig. 3I**).

To further elucidate these combinatorial regulatory interactions, we truncated ***y**R7 enh* to a 0.8 kb fragment (***y**R7 enh**) that recapitulated ***y**R7* expression driven by the entire ***y**R7 enh* fragment (**Fig. 3J, 3L, S3A**). Three other truncations that encompass the 0.8 kb region also recapitulated **y**R7 expression, while two truncations and four GAL4 lines generated by Janelia Research Campus and VDRC that excluded ***y**R7 enh** failed to drive GFP expression, consistent with the role of ***y**R7 enh** in driving **y**R7 specific expression (**Fig. 3J**). ***y**R7 enh** contains three conserved Ss binding sites (called Xenobiotic Response Elements/XREs) (**Fig. 3K**), consistent with regulation by Ss.

*weak **y**R7 enh* drove weak GFP expression in **y**R7s, co-localizing with Ss expression (**Fig. S1M-O**). *weak **y**R7 enh* and ***y**R7 enh** share a ~250 bp overlap that contains one of the three Ss XRE binding sites (**Fig. 3J-K**), suggesting that while the shared XRE site can drive GFP in **y**R7s, strong expression requires the presence of additional XRE sites. The Janelia enhancer GMR42E10 shares a ~75 bp overlap with ***y**R7 enh* but does not contain any Ss XRE binding sites (**Fig. 3J-K**). This construct failed to drive GFP expression, suggesting that at least one Ss XRE binding site is required for **y**R7-specific expression.

To further test the roles of Ss XRE binding sites, we generated a ***y**R7 enh** construct that replaces all GCGTG Ss XRE binding sites with AAAAA. This construct showed a near complete loss of **y**R7 GFP expression, indicating the importance of these sites for Ss activation (**Fig. 3M**). Very low-level expression of this reporter suggests the presence of additional cryptic Ss sites within ***y**R7 enh** (**Fig. 3M**). Searching ***y**R7 enh** for low affinity Ss binding motifs (Zhu et al., 2011), we identified two putative sites (GTCTGA and GTGTGA), one of which is conserved (GTCTGA), suggesting that these cryptic/low affinity sites may drive very low level expression in the absence of core, conserved (GCGTG) sites. Together, these data suggest that Ss directly binds the XRE sites in ***y**R7 enh** to regulate expression. However, we cannot rule out possible indirect mechanisms.

While ***y**R7 enh** has three Ss XRE sites, this enhancer contains no predicted Sal sites (Barrio et al., 1996; Sanchez et al., 2011), suggesting that Sal regulates ***y**R7 enh** either directly via binding to cryptic sites or indirectly through regulation of other intermediary factors. The longer ***y**R7 enh* contains a Sal binding site, which may contribute to regulation. Genetic epistasis analysis supports an indirect mode of regulation by Sal (**Fig. S4**; see below).

***y**R7 enh** is required for expression of endogenous Dve in **y**R7s, since CRISPR-generated deletion of ***y**R7 enh** caused a loss of Dve expression specifically in R7s (**Fig. 2A, 3N**) and a corresponding upregulation of Rh3 in all PRs (**Fig. 3O**). Similarly, the larger *dve*^{exel} deletion, covering ***y**R7 enh* and the *dve-A* promoter*,* also resulted in Rh3 upregulation in R7s (**Fig. 2A, S1G**).

Together, these results suggest that **y**R7-specfic expression of Dve requires ***y**R7 enh*, whose activation is mediated by Ss, Sal, and Otd.

Negative feedback onto *yR7 enh* determines homeostatic levels

Expression levels of Dve are precisely controlled to determine region-specific activation or repression of Rh3 in **y**R7s (Thanawala et al., 2013) (**Fig. 1D**). Negative feedback is a mechanism that ensures precise, homeostatic levels of gene expression. Since Dve is a transcriptional repressor, we hypothesized that Dve feeds back onto ***y**R7 enh* to control expression levels. To test Dve for negative regulation of ***y**R7 enh*, Dve was expressed in all PRs at high levels causing a complete loss of ***y**R7 enh* expression (**Fig. 4A**). ***y**R7 enh* was expressed at higher levels in **y**R7s in *dve* mutant clones compared to wild type clones (**Fig. 4B-C, 4F**), suggesting that Dve driven by ***y**R7 enh* feeds back to control levels of expression in **y**R7s (**Fig. 4H**).

yR7 enh **is a "dark" shadow enhancer for outer PR expression**

In addition to **y**R7s, expression of ***y****R7 enh* occurred in outer PRs in *dve* mutant clones (**Fig. 4D-E, 4G**), suggesting that *outer enh* induces Dve expression to completely repress ***y****R7 enh* in outer PRs in normal conditions (**Fig. 4I-J**). Since ***y****R7 enh* was never expressed in **p**R7s or R8s in wild type or in *dve* mutants (**Fig. 4B-E**), ***y****R7 enh* is only competent to drive expression in **y**R7s and outer PRs, where Dve is normally expressed.

Since *outer enh* drives expression in outer PRs in normal conditions and ***y****R7 enh* drives expression in outer PRs in *dve* mutants, we predicted that deleting *outer enh* would cause ***y****R7 enh* to drive expression of endogenous *dve* in outer PRs (**Fig. 4I-J**). Flies with CRISPR-mediated deletion of *outer enh* displayed expression of Dve in outer PRs (**Fig. 4K**) and repression of Rh3, Rh5, and Rh6 (i.e. Dve target genes) in outer PRs in 1 week old adults (**Fig. 4L, N**), suggesting that ***y****R7 enh* drives expression in the absence of functional *outer enh.* While Rh3 expression remained unchanged (**Fig. 4M**), variable derepression of Rh5 and Rh6 occurred in 4 week old adults (**Fig. 4O**), suggesting that expression driven by ***y****R7 enh* is not sufficient to completely rescue Dve expression due to differences in levels or timing.

Since ***y****R7 enh* can drive expression in outer PRs, ***y****R7 enh* is a shadow enhancer (i.e. redundant regulatory DNA element) for *outer enh*, the primary enhancer for outer PR expression. Unlike typical shadow enhancers, the ***y****R7 enh* shadow enhancer is repressed ("dark") in outer PRs under normal conditions due to negative feedback from the primary enhancer (**Fig. 4I**). We therefore define ***y****R7 enh* as a "dark" shadow enhancer, since its expression in outer PRs only occurs when *outer enh* function is lost (**Fig. 4J**).

Otd/Dve sites play context-dependent roles in *yR7 enh*

Since Otd activates and Dve represses ***y**R7 enh,* we next tested the regulatory roles of canonical Otd/Dve binding sites (also called K50 sites; TAATCC). ***y**R7 enh** contains two Otd/Dve sites, which are perfectly conserved across at least 5 of 6 Drosophila species (**Fig. 3K**). Replacing these two sites with AAAAAA caused increased levels of GFP expression in **y**R7s (**Fig. 4P**), suggesting that these sites mediate repression by Dve but not activation by Otd in **y**R7s. Since Otd is required for expression of ***y**R7 enh*, the expression of GFP in **y**R7s in the absence of optimal Otd binding sites suggests that Otd may act through additional Otd-specific cryptic sites or that activation is mediated by another activator downstream of Otd. Mutation of these sites did not cause de-repression in outer PRs, suggesting that these sites mediate both repression by Dve and activation by Otd in outer PRs.

To test if Dve directly binds the two Otd/Dve sites in ***y**R7 enh*,* we conducted *in vitro* electrophoretic mobility shift assays (EMSAs). Dve bound sequences containing the Otd/Dve sites, and mutation of these sites dramatically decreased binding (**Fig. 4Q**), suggesting that Dve directly binds the two Otd/Dve sites in ***y**R7 enh** to repress expression.

Since regulation of ***y**R7 enh** is dependent on Otd/Dve sites, Otd likely directly binds these sites to regulate expression. However, we cannot rule out possible indirect mechanisms.

outer enh is activated by Otd and repressed by Sal

We next characterized *outer enh*, the primary enhancer for Dve expression in outer PRs (**Fig. 5A**). The *dve*^{exel} deletion, which removes the first exon of *dve,* the *dve-A* promoter, and ***y****R7 enh*, showed no derepression of Dve target genes (Rh3, Rh5 and Rh6) in outer PRs (**Fig. 2A, S1G**), suggesting that *outer enh* is sufficient to drive Dve expression in outer PRs.

Otd activates Dve expression in all PRs and Sal represses Dve expression in inner PRs (Johnston et al., 2011). *outer enh* expression was completely lost in *otd* mutants, consistent with a general requirement of Otd for *dve* expression (**Fig. 5B**). In *sal* mutants, *outer enh* was derepressed in inner PRs (**Fig. 5C**) suggesting that Sal represses this element in inner PRs. Ectopic expression of Ss in all PRs did not affect *outer enh* expression, consistent with regulation of this element independent of Ss (**Fig. 5D**). Thus, combinatorial regulation involving activation by Otd in all PRs and repression by Sal in inner PRs yields the outer PR-specific expression of *outer enh* (**Fig. 5E**).

We truncated *outer enh* to a 1.3kb fragment (*outer enh**) that recapitulated the expression of the entire *outer enh* fragment (**Fig. 2A, 5A, 5F, 5H, S3B**). Two larger truncations and a Janelia GAL4 construct (GMR40E08) that encompass this 1.3kb region also recapitulated expression, while fragments that exclude *outer enh** failed to drive GFP, consistent with the role of *outer enh** in driving outer PR-specific expression (**Fig. 5F**).

*outer enh** has four K50 homeodomain consensus sites (TAATCC) for Otd and Dve (**Fig. 5G**) (Chaney et al., 2005). *all PR enh 4* shares a 390 bp overlap with *outer enh**, including one of the Otd/Dve binding sites, suggesting that its weak expression in all PRs may be due to the single Otd/Dve binding site functioning independently from the repressive Sal input that regulates the entire *outer enh*.*

We generated an *outer enh** construct that removes all TAATCC Otd/Dve binding sites by replacing them with AAAAAA (**Fig. 5I**). This construct showed a near complete loss of GFP expression in outer PRs, consistent with our model that Otd is required for *outer enh* activation. Since regulation of *outer enh** is dependent on Otd/Dve sites, Otd likely directly binds these sites to regulate expression. However, we cannot rule out possible indirect mechanisms.

While *outer enh** has four Otd/Dve sites, this enhancer contains no predicted Sal sites (Barrio et al., 1996; Sanchez et al., 2011), suggesting that Sal regulates *outer enh** either directly via binding to cryptic sites or indirectly through regulation of other intermediary factors. The longer *outer enh* contains a Sal binding site, which may contribute to regulation.

Feedback onto *outer enh* determines homeostatic levels

Since ***y****R7 enh* is controlled by negative autoregulation, we next tested whether feedback also determines expression levels driven by *outer enh.* Since *outer enh* (and Dve) are highly expressed in outer PRs, we expected that *dve* mutants may exhibit subtle increases in expression from *outer enh*. Indeed, in *dve* mutant clones, *outer enh* was expressed at higher levels in outer PRs compared to wild type clones (**Fig. 6B-D**). To confirm negative feedback onto *outer enh,* Dve was ectopically expressed in all PRs at high levels (*all PRs>dve*), causing a complete loss of *outer enh* expression (**Fig. 6A**).

Thus, Dve driven by *outer enh* feeds back onto this enhancer to autoregulate and ensure homeostatic levels of expression in outer PRs (**Fig. 6E**).

To test if Dve directly binds the four Otd/Dve sites in *outer enh*,* we conducted EMSAs. Dve bound sequences containing the Otd/Dve sites, and mutation of these sites dramatically decreased binding (**Fig. 6F**), suggesting that Dve directly binds the four Otd/Dve sites in *outer enh** to repress expression.

Sal represses *outer enh* to allow Ss-mediated activation of *yR7 enh*

***y**R7 enh* is highly sensitive to levels of Dve feedback, particularly in outer PRs where Dve levels are high. Ss alone is sufficient to induce ***y**R7 enh* expression at high levels in all R7s but not outer PRs (**Fig. 3E**). Ss and Sal together are sufficient to induce ***y**R7 enh* at high levels in outer PRs (**Fig. 3H**). Since Dve driven by *outer enh* feeds back to repress ***y**R7 enh* in outer PRs (**Fig. 4D-E, 4I-J**) and Sal represses Dve expression from *outer enh* (**Fig. 5C**), Sal may activate ***y**R7 enh* by repressing *outer enh*.

One prediction of this model is that ectopic Ss should be sufficient to activate ***y**R7 enh* at high levels in outer PRs in the absence of Dve. Indeed, when Ss is expressed at high levels in all PRs in *otd* mutants that lack Dve (Johnston et al., 2011), ***y**R7 enh* is activated in all PRs (**Fig. S4A**).

This result highlights two facets of ***y**R7 enh* regulation. First, Ss activates ***y**R7 enh*, whereas Sal represses *outer enh* to allow expression of ***y**R7 enh*, suggesting that Sal interacts indirectly with ***y**R7 enh* (**Fig. S4B**). Second, Ss requires Otd to activate ***y**R7 enh* in wild type conditions (**Fig. 3B**) where Ss levels are low, while high levels of Ss are sufficient to override the requirement for Otd (**Fig. S4A**).

Discussion

Dve is expressed in an intricate pattern with distinct levels in different photoreceptors. The regulation required to achieve this pattern is complex, involving two enhancers controlled by three main mechanisms: combinatorial transcription factor input, negative feedback, and enhancer redundancy (**Fig. 7**). PR-specific Otd, inner PR-specific Sal, and **y**R7-specific Ss work together to induce expression of ***y**R7 enh* in **y**R7s (**Fig. 7A**). In contrast, Otd activates *outer enh* while Sal represses this enhancer to yield expression in outer photoreceptors (**Fig. 7B**).

Once these cell-type-specific patterns are set, negative feedback by Dve maintains expression of the two enhancers at distinct levels important for regulation of downstream *rhodopsin* genes (**Fig. 7C-D**). This negative feedback appears especially critical for the ***y**R7 enh*, whose expression levels determine activation or repression of Rh3 in different regions of the retina. Gene regulatory network motifs involving negative feedback minimize variation in expression levels. With negative feedback, high concentrations of a regulator repress its expression, while low levels allow its activation. Negative feedback thus ensures homeostatic levels of expression (Alon, 2007; Becskei and Serrano, 2000; Irvine et al., 1993; Stewart et al., 2013).

As an additional layer of regulation, *outer enh* drives high levels of Dve that repress ***y**R7 enh* in outer PRs (**Fig. 7E**). When *outer enh* function is lost, ***y**R7 enh* becomes active in outer PRs, functioning as a shadow enhancer to provide redundancy and robustness to expression (**Fig. 7F**). Complex multi-enhancer systems enable genes to integrate multiple regulatory inputs, yielding intricate expression patterns. While some enhancers account for distinct aspects of regulation, others drive overlapping patterns.

Shadow enhancers can compensate for removal of a primary enhancer, resulting in mostly unaltered gene expression (Hong et al., 2008; Miller et al., 2014; Nolte et al., 2013; Perry et al., 2012). These shadow enhancers provide reliability and robustness in pattern formation, allowing critical patterning genes to be resilient to environmental and genetic variation (Barolo, 2012; Bothma et al., 2015; Frankel et al., 2010; Perry et al., 2010).

We define ***y**R7 enh* as a dark shadow enhancer, since it is normally repressed in outer PRs but becomes active when the function of the primary enhancer is impaired. We were able to identify the ***y**R7 enh* dark shadow enhancer since we were characterizing how a complex pattern was controlled by combinatorial transcription factor input and feedback acting on two enhancers. Similar to the generality of shadow enhancers (Cannavo et al., 2016), dark shadow enhancers may be a common mechanism to ensure gene expression. However, they would be challenging to identify since they are only active upon genetic or possibly environmental perturbation.

Dve is a transcriptional repressor (Johnston et al., 2011) that acts directly on ***y**R7 enh* in outer PRs to repress expression (**Fig. 4Q**). Generally, transcriptional repressors would likely act directly on dark shadow enhancers to repress them, poising them as backup systems. For transcriptional activators, more complex, indirect mechanisms would be required. For example, the primary enhancer could induce the activator to activate expression of a transcriptional repressor, which in turn could repress the dark shadow enhancer. Since dark shadow enhancers require feedback, they would likely only be found in genes encoding regulatory factors.

A key aspect of regulation by primary enhancers and dark shadow enhancers is their differential responsiveness to repression. For *outer enh*, normal Dve levels induce a slight decrease in expression. However, for ***y****R7 enh*, these same levels completely turn off expression in outer PRs. The difference may lie in activation by Otd: *outer enh* contains four Otd/Dve sites, whereas ***y****R7 enh* contains two (**Fig. 3K, 5G**). Since these sites mediate both activation by Otd and repression by Dve, cooperative action by the four sites in *outer enh* may drive stronger expression and prevent repression. Generally, the primary enhancer is expressed and must be significantly less susceptible to repression than the dark shadow enhancer, which is off.

Expression of Dve in outer PRs is seen in the mosquitos *Anopheles gambiae* and *Aedes aegypti* (Johnston et al., 2011), suggesting a conserved role in Rh regulation that has been maintained over 250 million years of evolution. However, expression of Rhs in R7s of mosquito species is regionalized in contrast to the stochastic pattern in *Drosophila* (Hu and Castelli-Gair, 1999), suggesting that different mechanisms have arisen to regulate Dve and Rh expression in R7s. Dark shadow enhancers may be an ancestral mechanism to ensure gene expression despite evolutionary changes. Further, they may allow the evolution of new functions like the expression of ***y****R7 enh* in R7s.

Dark shadow enhancers appear to provide robustness to gene expression, and may act as additional mechanisms of canalization (i.e. the ability for individuals in a population to produce similar phenotypes regardless of environmental or genetic perturbation) (Waddington, 1942). Buffering of gene expression occurs at the levels of *cis*-regulatory logic (Dunipace et al., 2013; Frankel et al., 2010; Hong et al., 2008; Staller et al., 2015; Wunderlich et al., 2015) and gene networks (Cassidy et al., 2013;

Lott et al., 2007; Manu et al., 2009). Dark shadow enhancers are an interesting integration of these mechanisms, whereby a primary enhancer induces expression of a factor that feeds back to repress a dark shadow enhancer. When expression from the primary enhancer is perturbed, this feedback is broken and the dark shadow enhancer becomes active. Thus, dark shadow enhancers are poised as backup mechanisms for proper gene regulation. As our understanding of complex multi-enhancer systems increases, it will be interesting to see the generality of dark shadow enhancers.

In conclusion, our studies show how two enhancers integrate combinatorial transcription factor input, negative autoregulation, and redundancy in *cis*-regulatory elements to determine robust levels of gene expression in photoreceptor neurons. These mechanisms likely play roles in the establishment and maintenance of gene expression levels in other neuronal subtypes.

Acknowledgements:

We are grateful to Steve Britt, Lily Jan, Yuh-Nung Jan, Hideki Nakagoshi, Charles Zuker, the Bloomington Stock Center and the Vienna Drosophila Resource Center (VDRC) for generously providing published fly stocks and antibodies. We thank Rejji Kuruvilla, Mike Levine, David Lorberbaum, Richard Mann and Alexandra Neuhaus-Follini for helpful comments on the manuscript. RJJ and SS were supported by NIH R01GM106090/NYU F7784-01. RJJ was supported by the Pew Scholar Award 00027373, March of Dimes Basil O’Connor Scholar Award 5-FY15-21, and NIH R01EY025598.

Experimental Procedures

See Supplemental Experimental Procedures

References

Alon, U., 2007. Network motifs: theory and experimental approaches. Nat Rev Genet 8, 450-461.

Barolo, S., 2012. Shadow enhancers: frequently asked questions about distributed cis-regulatory information and enhancer redundancy. Bioessays 34, 135-141.

Barrio, R., de Celis, J.F., Bolshakov, S., Kafatos, F.C., 1999. Identification of regulatory regions driving the expression of the Drosophila spalt complex at different developmental stages. Dev Biol 215, 33-47.

Barrio, R., Shea, M.J., Carulli, J., Lipkow, K., Gaul, U., Frommer, G., Schuh, R., Jackle, H., Kafatos, F.C., 1996. The spalt-related gene of Drosophila melanogaster is a member of an ancient gene family, defined by the adjacent, region-specific homeotic gene spalt. Dev Genes Evol 206, 315-325.

Becskei, A., Serrano, L., 2000. Engineering stability in gene networks by autoregulation. Nature 405, 590-593.

Bell, M.L., Earl, J.B., Britt, S.G., 2007. Two types of Drosophila R7 photoreceptor cells are arranged randomly: a model for stochastic cell-fate determination. J Comp Neurol 502, 75-85.

Bothma, J.P., Garcia, H.G., Esposito, E., Schlissel, G., Gregor, T., Levine, M., 2014. Dynamic regulation of eve stripe 2 expression reveals transcriptional bursts in living Drosophila embryos. Proc Natl Acad Sci U S A 111, 10598-10603.

Bothma, J.P., Garcia, H.G., Ng, S., Perry, M.W., Gregor, T., Levine, M., 2015. Enhancer additivity and non-additivity are determined by enhancer strength in the Drosophila embryo. Elife 4.

Brand, A.H., Perrimon, N., 1993. Targeted gene expression as a means of altering cell fates and generating dominant phenotypes. Development 118, 401-415.

Cannavo, E., Khoueiry, P., Garfield, D.A., Geeleher, P., Zichner, T., Gustafson, E.H., Ciglar, L., Korbel, J.O., Furlong, E.E., 2016. Shadow Enhancers Are Pervasive Features of Developmental Regulatory Networks. Curr Biol 26, 38-51.

Cassidy, J.J., Jha, A.R., Posadas, D.M., Giri, R., Venken, K.J., Ji, J., Jiang, H., Bellen, H.J., White, K.P., Carthew, R.W., 2013. miR-9a minimizes the phenotypic impact of genomic diversity by buffering a transcription factor. Cell 155, 1556-1567.

Chaney, B.A., Clark-Baldwin, K., Dave, V., Ma, J., Rance, M., 2005. Solution structure of the K50 class homeodomain PITX2 bound to DNA and implications for mutations that cause Rieger syndrome. Biochemistry 44, 7497-7511.

Chen, S.K., Badea, T.C., Hattar, S., 2011. Photoentrainment and pupillary light reflex are mediated by distinct populations of ipRGCs. Nature 476, 92-95.

Chou, W.H., Hall, K.J., Wilson, D.B., Wideman, C.L., Townson, S.M., Chadwell, L.V., Britt, S.G., 1996. Identification of a novel Drosophila opsin reveals specific patterning of the R7 and R8 photoreceptor cells. Neuron 17, 1101-1115.

Corty, M.M., Tam, J., Grueber, W.B., 2016. Dendritic diversification through transcription factor-mediated suppression of alternative morphologies. Development 143, 1351-1362.

Dasen, J.S., De Camilli, A., Wang, B., Tucker, P.W., Jessell, T.M., 2008. Hox repertoires for motor neuron diversity and connectivity gated by a single accessory factor, FoxP1. Cell 134, 304-316.

Duncan, D.M., Burgess, E.A., Duncan, I., 1998. Control of distal antennal identity and tarsal development in Drosophila by spineless-aristapedia, a homolog of the mammalian dioxin receptor. Genes Dev 12, 1290-1303.

Dunipace, L., Saunders, A., Ashe, H.L., Stathopoulos, A., 2013. Autoregulatory feedback controls sequential action of cis-regulatory modules at the brinker locus. Dev Cell 26, 536-543.

Fortini, M.E., Rubin, G.M., 1990. Analysis of cis-acting requirements of the Rh3 and Rh4 genes reveals a bipartite organization to rhodopsin promoters in Drosophila melanogaster. Genes Dev 4, 444-463.

Franceschini, N., Kirschfeld, K., Minke, B., 1981. Fluorescence of photoreceptor cells observed in vivo. Science 213, 1264-1267.

Frankel, N., Davis, G.K., Vargas, D., Wang, S., Payre, F., Stern, D.L., 2010. Phenotypic robustness conferred by apparently redundant transcriptional enhancers. Nature 466, 490-493.

Gao, S., Takemura, S.Y., Ting, C.Y., Huang, S., Lu, Z., Luan, H., Rister, J., Thum, A.S., Yang, M., Hong, S.T., Wang, J.W., Odenwald, W.F., White, B.H., Meinertzhagen, I.A., Lee, C.H., 2008. The neural substrate of spectral preference in Drosophila. Neuron 60, 328-342.

Grueber, W.B., Jan, L.Y., Jan, Y.N., 2003. Different levels of the homeodomain protein cut regulate distinct dendrite branching patterns of Drosophila multidendritic neurons. Cell 112, 805-818.

Hardie, R.C., 1985. Functional organization of the fly retina. In: Autrum H, Ottoson D, Perl ER, Schmidt RF, Shimazu H, Willis WD, editors.Progress in Sensory Physiology. . Springer, Berlin.

Hong, J.W., Hendrix, D.A., Levine, M.S., 2008. Shadow enhancers as a source of evolutionary novelty. Science 321, 1314.

Hsiao, H.Y., Johnston, R.J., Jukam, D., Vasiliauskas, D., Desplan, C., Rister, J., 2012. Dissection and immunohistochemistry of larval, pupal and adult Drosophila retinas. J Vis Exp, e4347.

Hsiao, H.Y., Jukam, D., Johnston, R., Desplan, C., 2013. The neuronal transcription factor erect wing regulates specification and maintenance of Drosophila R8 photoreceptor subtypes. Dev Biol 381, 482-490.

Hu, N., Castelli-Gair, J., 1999. Study of the posterior spiracles of Drosophila as a model to understand the genetic and cellular mechanisms controlling morphogenesis. Dev Biol 214, 197-210.

Irvine, K.D., Botas, J., Jha, S., Mann, R.S., Hogness, D.S., 1993. Negative autoregulation by Ultrabithorax controls the level and pattern of its expression. Development 117, 387-399.

Johnston, R.J., Jr., 2013. Lessons about terminal differentiation from the specification of color-detecting photoreceptors in the Drosophila retina. Ann N Y Acad Sci 1293, 33-44.

Johnston, R.J., Jr., Desplan, C., 2010. Stochastic mechanisms of cell fate specification that yield random or robust outcomes. Annu Rev Cell Dev Biol 26, 689-719.

Johnston, R.J., Jr., Desplan, C., 2014. Interchromosomal communication coordinates intrinsically stochastic expression between alleles. Science 343, 661-665.

Johnston, R.J., Jr., Otake, Y., Sood, P., Vogt, N., Behnia, R., Vasiliauskas, D., McDonald, E., Xie, B., Koenig, S., Wolf, R., Cook, T., Gebelein, B., Kussell, E., Nakagoshi, H., Desplan, C., 2011. Interlocked feedforward loops control cell-type-specific Rhodopsin expression in the Drosophila eye. Cell 145, 956-968.

Jukam, D., Desplan, C., 2011. Binary regulation of Hippo pathway by Merlin/NF2, Kibra, Lgl, and Melted specifies and maintains postmitotic neuronal fate. Dev Cell 21, 874-887.

Jukam, D., Viets, K., Anderson, C., Zhou, C., DeFord, P., Yan, J., Cao, J., Johnston, R.J., Jr., 2016. The insulator protein BEAF-32 is required for Hippo pathway activity in the terminal differentiation of neuronal subtypes. Development 143, 2389-2397.

Jukam, D., Xie, B., Rister, J., Terrell, D., Charlton-Perkins, M., Pistillo, D., Gebelein, B., Desplan, C., Cook, T., 2013. Opposite feedbacks in the Hippo pathway for growth control and neural fate. Science 342, 1238016.

Kuhnlein, R.P., Schuh, R., 1996. Dual function of the region-specific homeotic gene spalt during Drosophila tracheal system development. Development 122, 2215-2223.

Li-Kroeger, D., Witt, L.M., Grimes, H.L., Cook, T.A., Gebelein, B., 2008. Hox and senseless antagonism functions as a molecular switch to regulate EGF secretion in the Drosophila PNS. Dev Cell 15, 298-308.

Lott, S.E., Kreitman, M., Palsson, A., Alekseeva, E., Ludwig, M.Z., 2007. Canalization of segmentation and its evolution in Drosophila. Proc Natl Acad Sci U S A 104, 10926-10931.

Manu, Surkova, S., Spirov, A.V., Gursky, V.V., Janssens, H., Kim, A.R., Radulescu, O., Vanario-Alonso, C.E., Sharp, D.H., Samsonova, M., Reinitz, J., 2009. Canalization of gene expression in the Drosophila blastoderm by gap gene cross regulation. PLoS Biol 7, e1000049.

Mazzoni, E.O., Celik, A., Wernet, M.F., Vasiliauskas, D., Johnston, R.J., Cook, T.A., Pichaud, F., Desplan, C., 2008. Iroquois complex genes induce co-expression of rhodopsins in Drosophila. PLoS Biol 6, e97.

Mikeladze-Dvali, T., Wernet, M.F., Pistillo, D., Mazzoni, E.O., Teleman, A.A., Chen, Y.W., Cohen, S., Desplan, C., 2005. The growth regulators warts/lats and melted interact in a bistable loop to specify opposite fates in Drosophila R8 photoreceptors. Cell 122, 775-787.

Miller, S.W., Rebeiz, M., Atanasov, J.E., Posakony, J.W., 2014. Neural precursor-specific expression of multiple Drosophila genes is driven by dual enhancer modules with overlapping function. Proc Natl Acad Sci U S A 111, 17194-17199.

Mollereau, B., Dominguez, M., Webel, R., Colley, N.J., Keung, B., de Celis, J.F., Desplan, C., 2001. Two-step process for photoreceptor formation in Drosophila. Nature 412, 911-913.

Nakagawa, Y., Fujiwara-Fukuta, S., Yorimitsu, T., Tanaka, S., Minami, R., Shimooka, L., Nakagoshi, H., 2011. Spatial and temporal requirement of defective proventriculus activity during Drosophila midgut development. Mech Dev 128, 258-267.

Nakagoshi, H., Hoshi, M., Nabeshima, Y., Matsuzaki, F., 1998. A novel homeobox gene mediates the Dpp signal to establish functional specificity within target cells. Genes Dev 12, 2724-2734.

Nolte, C., Jinks, T., Wang, X., Martinez Pastor, M.T., Krumlauf, R., 2013. Shadow enhancers flanking the HoxB cluster direct dynamic Hox expression in early heart and endoderm development. Dev Biol 383, 158-173.

O'Gorman, S., Fox, D.T., Wahl, G.M., 1991. Recombinase-mediated gene activation and site-specific integration in mammalian cells. Science 251, 1351-1355.

Perry, M.W., Boettiger, A.N., Bothma, J.P., Levine, M., 2010. Shadow enhancers foster robustness of Drosophila gastrulation. Curr Biol 20, 1562-1567.

Perry, M.W., Bothma, J.P., Luu, R.D., Levine, M., 2012. Precision of hunchback expression in the Drosophila embryo. Curr Biol 22, 2247-2252.

Sanchez, J., Talamillo, A., Gonzalez, M., Sanchez-Pulido, L., Jimenez, S., Pirone, L., Sutherland, J.D., Barrio, R., 2011. Drosophila Sal and Salr are transcriptional repressors. Biochem J 438, 437-445.

Smith, C.J., O'Brien, T., Chatzigeorgiou, M., Spencer, W.C., Feingold-Link, E., Husson, S.J., Hori, S., Mitani, S., Gottschalk, A., Schafer, W.R., Miller, D.M., 3rd, 2013. Sensory neuron fates are distinguished by a transcriptional switch that regulates dendrite branch stabilization. Neuron 79, 266-280.

Sood, P., Johnston, R.J., Jr., Kussell, E., 2012. Stochastic de-repression of Rhodopsins in single photoreceptors of the fly retina. PLoS Comput Biol 8, e1002357.

Staller, M.V., Vincent, B.J., Bragdon, M.D., Lydiard-Martin, T., Wunderlich, Z., Estrada, J., DePace, A.H., 2015. Shadow enhancers enable Hunchback bifunctionality in the Drosophila embryo. Proc Natl Acad Sci U S A 112, 785-790.

Stewart, A.J., Seymour, R.M., Pomiankowski, A., Reuter, M., 2013. Under-dominance constrains the evolution of negative autoregulation in diploids. PLoS Comput Biol 9, e1002992.

Tahayato, A., Sonneville, R., Pichaud, F., Wernet, M.F., Papatsenko, D., Beaufils, P., Cook, T., Desplan, C., 2003. Otd/Crx, a dual regulator for the specification of ommatidia subtypes in the Drosophila retina. Dev Cell 5, 391-402.

Terriente, J., Perea, D., Suzanne, M., Diaz-Benjumea, F.J., 2008. The Drosophila gene zfh2 is required to establish proximal-distal domains in the wing disc. Dev Biol 320, 102-112.

Thanawala, S.U., Rister, J., Goldberg, G.W., Zuskov, A., Olesnicky, E.C., Flowers, J.M., Jukam, D., Purugganan, M.D., Gavis, E.R., Desplan, C., Johnston, R.J., Jr., 2013. Regional modulation of a stochastically expressed factor determines photoreceptor subtypes in the Drosophila retina. Dev Cell 25, 93-105.

Vandendries, E.R., Johnson, D., Reinke, R., 1996. orthodenticle is required for photoreceptor cell development in the Drosophila eye. Dev Biol 173, 243-255.

Viets, K., Eldred, K.C., Johnston, R.J., Jr., 2016. Mechanisms of Photoreceptor Patterning in Vertebrates and Invertebrates. Trends Genet 32, 638-659.

Waddington, C.H., 1942. Canalization of development and the inheritance of acquired characteristics. Nature 150, 563-565.

Wernet, M.F., Labhart, T., Baumann, F., Mazzoni, E.O., Pichaud, F., Desplan, C., 2003. Homothorax switches function of Drosophila photoreceptors from color to polarized light sensors. Cell 115, 267-279.

Wernet, M.F., Mazzoni, E.O., Celik, A., Duncan, D.M., Duncan, I., Desplan, C., 2006. Stochastic spineless expression creates the retinal mosaic for colour vision. Nature 440, 174-180.

Wolff, T., Ready, D.F., 1993. Pattern formation in the Drosophila retina. In: BATE M, MARTINEZ-ARIAS A, editors. The development of Drosophila melanogaster. II. Cold Spring Harbor Laboratory Press, Cold Spring Harbor, 1277–1316.

Wunderlich, Z., Bragdon, M.D., Vincent, B.J., White, J.A., Estrada, J., DePace, A.H., 2015. Kruppel Expression Levels Are Maintained through Compensatory Evolution of Shadow Enhancers. Cell Rep 12, 1740-1747.

Yamaguchi, S., Desplan, C., Heisenberg, M., 2010. Contribution of photoreceptor subtypes to spectral wavelength preference in Drosophila. Proc Natl Acad Sci U S A 107, 5634-5639.

Zhu, L.J., Christensen, R.G., Kazemian, M., Hull, C.J., Enuameh, M.S., Basciotta, M.D., Brasefield, J.A., Zhu, C., Asriyan, Y., Lapointe, D.S., Sinha, S., Wolfe, S.A., Brodsky, M.H., 2011.

FlyFactorSurvey: a database of Drosophila transcription factor binding specificities determined using the bacterial one-hybrid system. Nucleic Acids Res 39, D111-117.

Figures

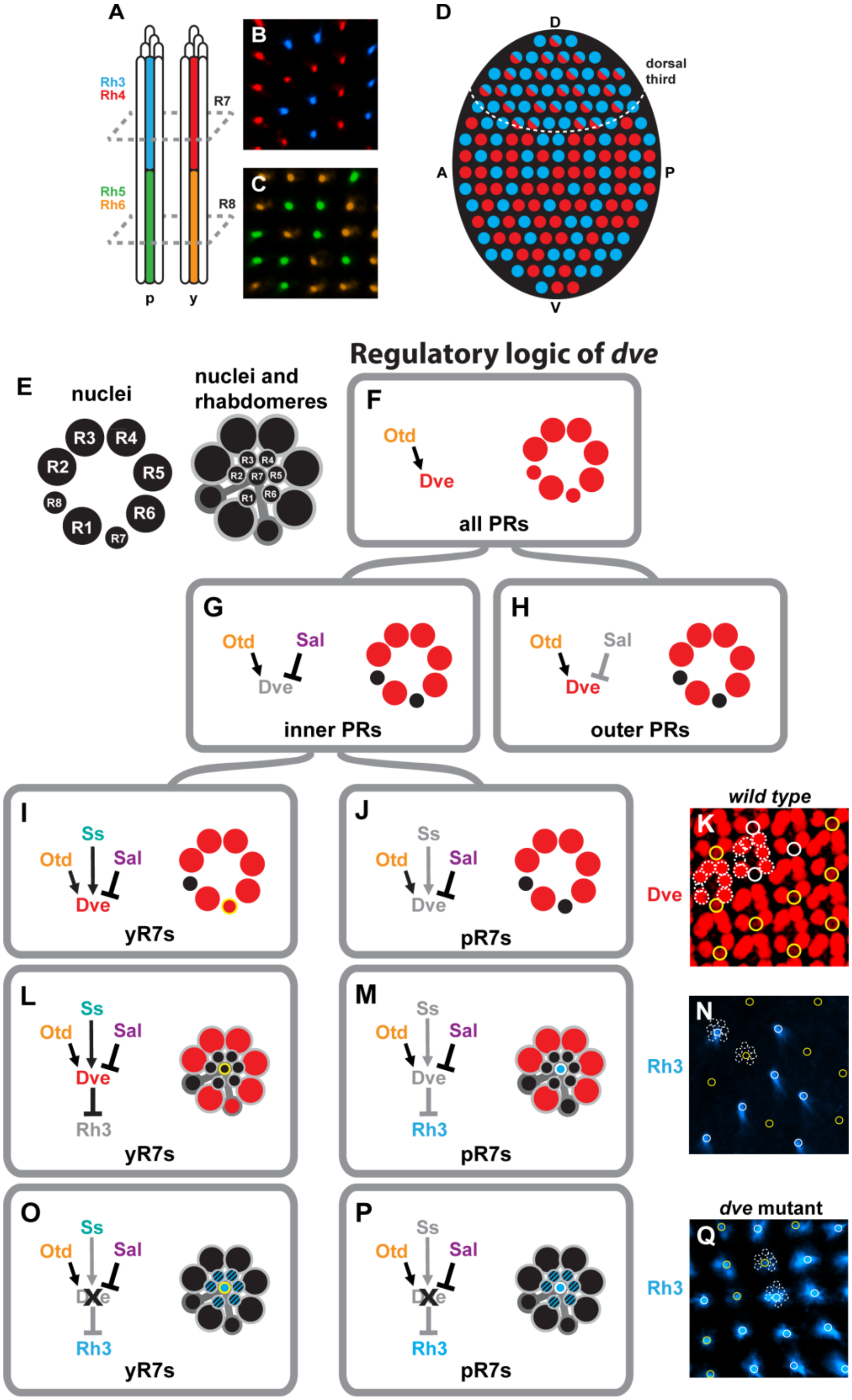
A
Rh3
Rh4
R7
Rh5
Rh6
R8
p
y
B
C
D
dorsal third
A
P
V
E
nuclei
R3
R4
R2
R5
R8
R6
R1
R7
nuclei and rhabdomeres
Regulatory logic of *dve*
F
Otd
Dve
all PRs
G
Otd
Sal
Dve
inner PRs
H
Otd
Sal
Dve
outer PRs
I
Ss
Otd
Sal
Dve
yR7s
J
Ss
Otd
Sal
Dve
pR7s
wild type
K
Dve
L
Ss
Otd
Sal
Dve
Rh3
yR7s
M
Ss
Otd
Sal
Dve
Rh3
pR7s
N
Rh3
O
Ss
Otd
Sal
Dve
Rh3
yR7s
P
Ss
Otd
Sal
Dve
Rh3
pR7s
dve mutant
Q
Rh3

Figure 1. The regulatory logic controlling Dve

A. Schematic of Rh3 (blue) and Rh4 (red) expression in **p** and **y**R7s coordinating with Rh5 (green) and Rh6 (orange) expression in **p** and **y**R8s in adults. B-C. Rh3, Rh4, Rh5, and Rh6 in cross-sectional view depicted by gray dashed lines in A. Images were taken in adult flies.

D. In the adult fly eye, two ommatidial subtypes, the Rh3-expressing **p**R7s (blue circles) and the Rh4-expressing **y**R7s (red circles), are randomly distributed in the retina at a ratio of 35:65. This mutual exclusivity in expression breaks down in the dorsal third region, where Rh3 and Rh4 are co-expressed in the **y** subtype (half red/half blue circles). A: anterior; P: posterior; D: dorsal; V: ventral.

E. Schematic of nuclei and rhabdomeres of the 8 PRs (R1-8) that make up the fly ommatidium. Large, black circles on the outside represent nuclei, while smaller inner circles represent rhabdomeres.

For F-J, L-M, and O-P, Regulatory logic governing *dve*. Left: gene network; right: Dve expression pattern. Solid color represents consistent expression. Crosshatched colors indicate variable, derepressed expression.

F. Otd activates Dve in all PRs.

G. Sal represses Dve in inner PRs.

H. The absence of Sal allows Dve expression in outer PRs.

I. Ss activates Dve in **y**R7s.

J. The absence of Ss prevents Dve expression in **p**R7s.

K. The interactions in F-J yield the expression pattern of Dve: high expression in outer PRs, low expression in **y**R7s, and no expression in **p**R7s and R8s in pupae. Yellow circles indicate **y**R7 nuclei with *dve* on, solid white circles indicate **p**R7 nuclei with *dve* off, and dashed white circles are nuclei of outer PRs and R8s.

For N, Q. Yellow circles indicate **y**R7 rhabdomeres. Solid white circles indicate **p**R7 rhabdomeres. Dashed white circles are rhabdomeres of outer PRs.

L. Dve represses Rh3 in **y**R7s.

M. The absence of Dve allows Rh3 expression in **p**R7s.

N. Rh3 is expressed only in **p**R7s where Dve is absent in adults.

O-Q. In *dve* mutants, Rh3 is expressed in all R7s and variably derepressed in outer PRs in adults.

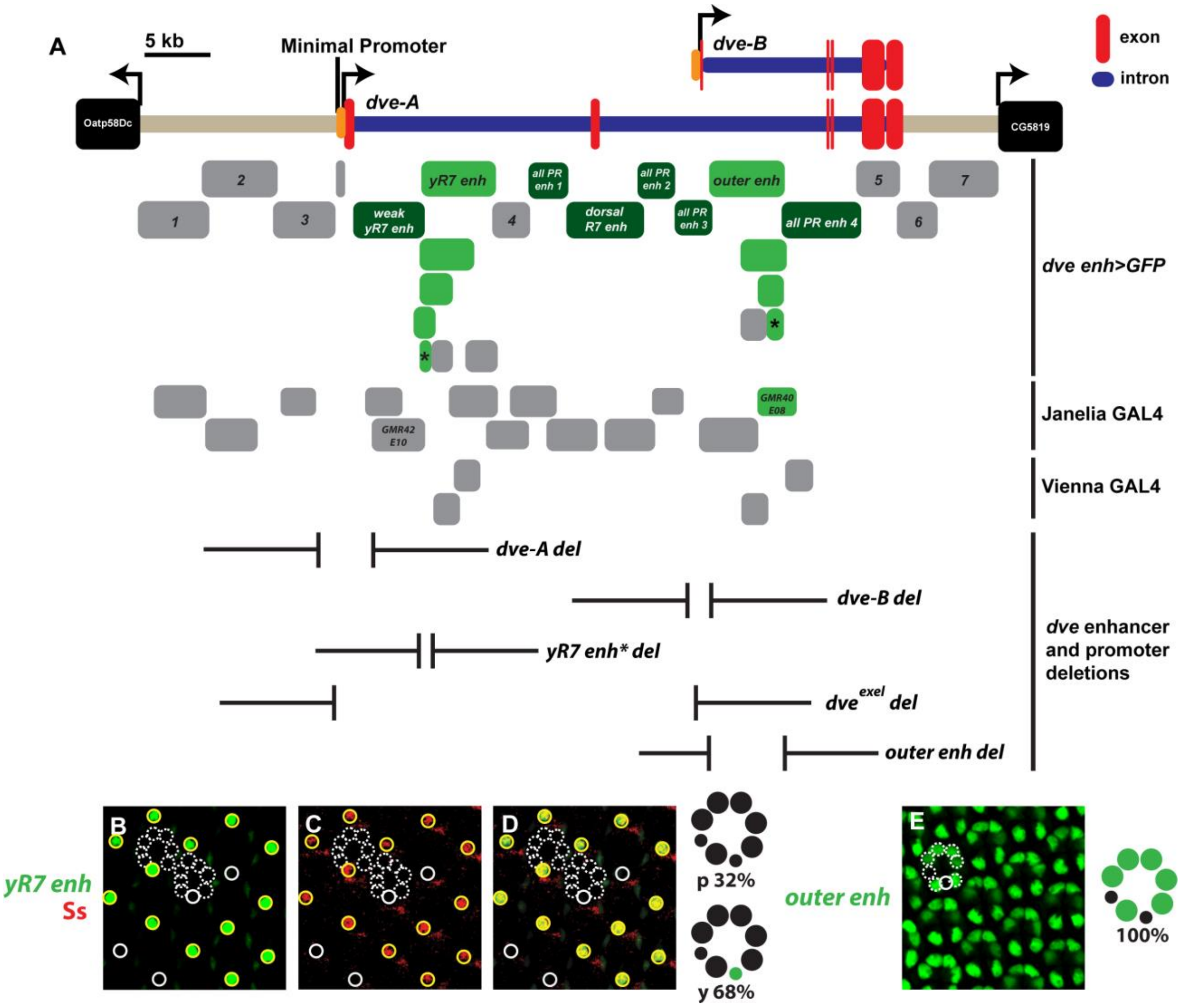

Figure 2. Two enhancers recapitulate Dve expression

A. Schematic representation of the *dve* locus, reporter constructs, and deletions. Reporter constructs (*dve enh>GFP*) consist of fragments of the *dve* locus and the *dve-A* promoter driving nuclear GFP. Smaller fragments denoted with * represent truncations that recapitulate the expression level of the original *dve enh>GFP* constructs. Janelia Research Campus and VDRC stocks contain fragments of the *dve* locus driving Gal4. Light green fragments drove strong expression. Dark green fragments drove weak expression. Gray fragments did not drive expression.

B-D. ***y**R7 enh* drove expression in **y**R7s at mid-pupation; Ss is a marker for **y**R7s. Yellow circles indicate **y**R7 cells; solid white circles indicate **p**R7 cells; dashed white circles are outer PRs and R8s. In schematics, black circles indicate no GFP expression and green circle indicates GFP expression. Note: Figure 2B and Figure 3A are the same image, reproduced in both figures for ease of reading.

E. *outer enh* constructs drove GFP expression in outer PRs at mid-pupation. Dashed white circles indicate outer PRs and R8s; solid white circle indicates R7.

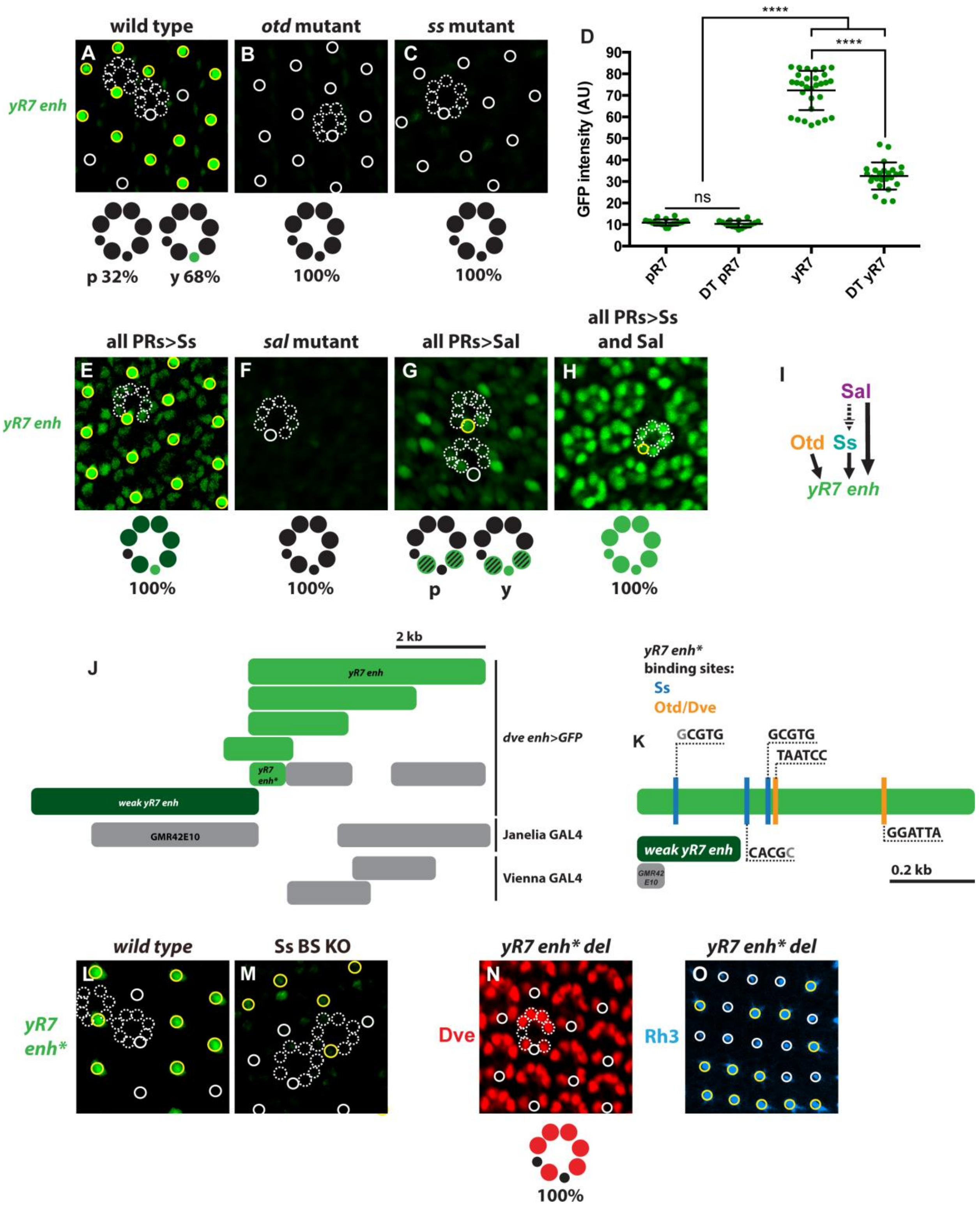
wild type
otd mutant
ss mutant
yR7 enh
A
B
C
p 32%
y 68%
100%
100%
D
****
****
ns
GFP intensity (AU)
0
10
20
30
40
50
60
70
80
90
pR7
DT pR7
yR7
DT yR7
all PRs>Ss
sal mutant
all PRs>Sal
all PRs>Ss and Sal
yR7 enh
E
F
G
H
100%
100%
p
y
100%
I
Sal
Otd
Ss
yR7 enh
2 kb
J
yR7 enh
yR7 enh*
weak yR7 enh
GMR42E10
dve enh>GFP
Janelia GAL4
Vienna GAL4
yR7 enh*
binding sites:
Ss
Otd/Dve
K
GCGTG
GCGTG
TAATCC
weak yR7 enh
CACGC
GGATTA
GMR42 E10
0.2 kb
wild type
Ss BS KO
yR7 enh* del
yR7 enh* del
yR7 enh*
L
M
N
O
Dve
Rh3
100%

Figure 3. *yR7 enh* is activated by Otd, Sal, and Ss

For A-C, E-H, L-M, yellow circles indicate **y**R7s; solid white circles indicate **p**R7s. Dashed white circles indicate outer PRs and R8s. Light green in ommatidium schematic indicates strong GFP expression; dark green indicates weak expression; crosshatch indicates variable expression; black indicates lack of expression. Images were acquired at mid-pupation.

A. ***y****R7 enh* is expressed in **y**R7s. Note: Figure 2B and Figure 3A are the same image, reproduced in both figures for ease of reading.

B. Expression of ***y****R7 enh* is lost in *otd* mutants.

C. Expression of ***y****R7 enh* is lost in *ss* mutants.

D. Quantification of GFP intensity in R7 cells shows three distinct intensity levels corresponding to **p**R7 (including **p**R7 and dorsal third (DT) **p**R7), **y**R7, and DT **y**R7 expression. Error bars are standard deviations of the mean. n=22 for **p**R7s, 16 for DT **p**R7s, 31 for **y**R7s, and 31 for DT **y**R7s. **** indicates $p < 0.0001$, ns indicates $p > 0.05$ and not significant, unpaired t test with Welch's correction. All measurements were internally controlled within a single mid-pupal retina.

E. ***y****R7 enh* is strongly expressed in all R7s and weakly expressed in all PRs when Ss is ectopically expressed in all PRs.

F. Expression of ***y****R7 enh* is lost in *sal* mutants (note: white circle indicates presumptive R7).

G. ***y****R7 enh* is expressed in random R1s and R6s when Sal is ectopically expressed in all PRs.

H. ***y****R7 enh* is expressed in all PRs when Ss and Sal are ectopically expressed in all PRs (note: yellow circle indicates presumptive **y**R7).

I. The regulatory interactions governing ***y****R7 enh.* Otd, Ss, and Sal activate ***y****R7 enh*, while Sal activates stochastic expression of Ss in **y**R7s (denoted by dashed arrow).

J. A truncated 0.8 kb fragment of ***y****R7 enh*, denoted ***y****R7 enh*,* was sufficient to recapitulate GFP expression in **y**R7 cells. Larger truncations encompassing ***y****R7 enh** also expressed GFP in **y**R7 cells, while truncations excluding ***y****R7 enh** did not drive GFP expression. *weak* ***y****R7 enh* shares a ~250 bp overlap with ***y****R7 enh**, including one of the three Ss XRE binding sites (**Fig. 3K**). GMR42E10, a construct generated by Janelia that contains a fragment of *dve* driving Gal4, shares a ~75 bp overlap with ***y****R7 enh* that does not contain any Ss XRE binding sites (**Fig. 3K**). This construct failed to drive GFP expression in **y**R7 cells. Light green fragments drove strong GFP expression, dark green fragments drove weak GFP expression, and gray fragments did not drive GFP expression.

K. ***y****R7 enh** contains three Ss binding sites and two Otd/Dve binding sites. Capitalized black text indicates perfect conservation across 6 *Drosophila* species. Capitalized gray indicates conservation across 5 of the 6 species. Light green fragments drove strong GFP expression, dark green fragments drove weak GFP expression, and gray fragments did not drive GFP expression.

L. ***y****R7 enh** is expressed in **y**R7s, similar to Dve and ***y****R7 enh*.

M. Knocking out Ss XRE binding sites in the ***y****R7 enh** construct resulted in a near complete loss of GFP expression. BS KO: binding site knockout.

N. CRISPR-mediated deletion of ***y****R7 enh* from the endogenous *dve* locus resulted in loss of Dve specifically in **y**R7s. Dashed white circles indicate outer PRs and R8s; solid white circles indicate R7s.

O. Loss of Dve in **y**R7s resulted in derepression of Rh3 in adults. Yellow circles indicate **y**R7s; white circles indicate **p**R7s.

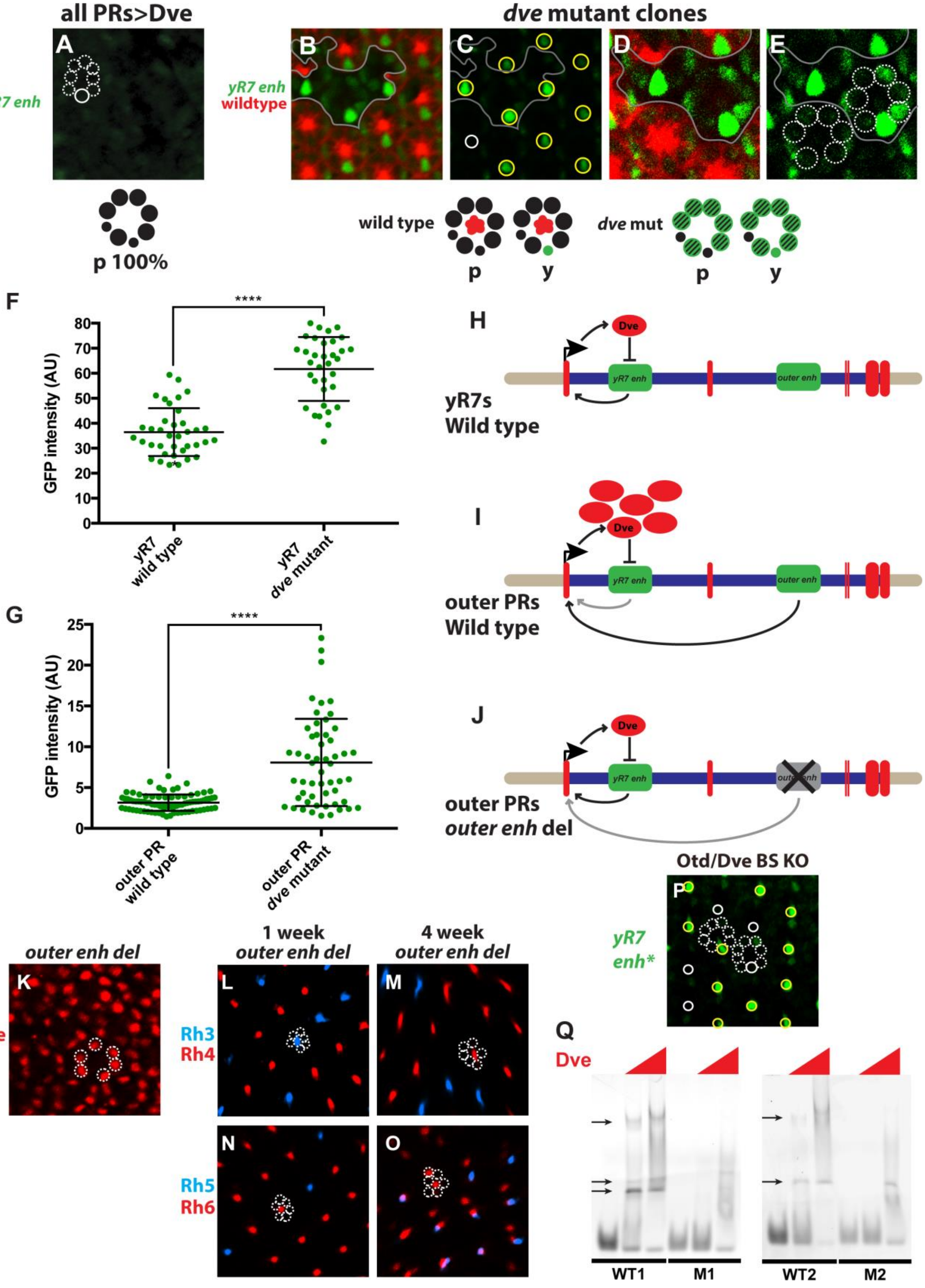
all PRs>Dve
A
yR7 enh
p 100%
dve mutant clones
B
C
D
E
yR7 enh
wildtype
wild type
p
y
dve mut
p
y
F
****
GFP intensity (AU)
0
10
20
30
40
50
60
70
80
yR7 wild type
yR7 dve mutant
G
****
GFP intensity (AU)
0
5
10
15
20
25
outer PR wild type
outer PR dve mutant
H
Dve
yR7 enh
outer enh
yR7s
Wild type
I
Dve
yR7 enh
outer enh
outer PRs
Wild type
J
Dve
yR7 enh
outer enh
outer PRs
outer enh del
outer enh del
K
Dve
1 week
outer enh del
4 week
outer enh del
L
M
Rh3
Rh4
N
O
Rh5
Rh6
Otd/Dve BS KO
P
yR7
enh*
Q
Dve
WT1
M1
WT2
M2

Figure 4. Dve feeds back to control *yR7 enh*

For A-E, expression analysis was conducted on mid-pupal retinas.

A. Expression of ***y****R7 enh* is lost when Dve is ectopically expressed in all PRs. Dashed white circles indicate outer PRs and R8s; solid white circle indicates R7. In schematic, black circles indicate no GFP expression.

For B-E, Yellow circles indicate **y**R7 cells; white circles indicate **p**R7 cells. Dashed white circles are outer PRs. Solid gray line represents boundary between *dve* mutant clones (indicated by absence of RFP) and wild type clones (indicated by presence of RFP). Bright green in ommatidium schematic indicates strong GFP expression; crosshatch indicates variable expression; black indicates lack of expression; red spot indicates RFP expression.

B-C. In **y**R7s, ***y****R7 enh* is upregulated in *dve* mutant clones compared to wild type clones.

D-E. In outer PRs, ***y****R7 enh* is upregulated in *dve* mutant clones compared to wild type clones.

F. Quantification of **y**R7 GFP intensity in *dve* mutant and wild type clones. **y**R7s in *dve* mutants show greater GFP intensity than in wild type clones. R7 cells with GFP on indicate **y**R7s. n= 37 for wild type **y**R7s and n= 37 for *dve* mutant **y**R7s.**** indicates $p< 0.0001$, unpaired t test with Welch's correction. All measurements were internally controlled within a single mid-pupal retina.

G. Quantification of GFP intensity of outer PRs in *dve* mutant and wild type clones. In wild type clones, outer PRs are GFP off, while *dve* mutant clones show a much greater distribution of GFP expression states. n=84 for wild type outer PRs and n=54 for *dve* mutant outer PRs. **** indicates p <0.0001, unpaired t test with Welch's correction. All measurements were internally controlled within a single mid-pupal retina.

H. ***y****R7 enh* induces Dve expression that negatively feeds back onto ***y****R7 enh* to maintain homeostatic Dve levels in **y**R7 cells.

I. *outer enh* induces Dve expression that negatively feeds back onto ***y****R7 enh* to completely repress ***y****R7* expression in outer PRs.

J. When *outer enh* function is impaired, ***y****R7 enh* is derepressed in outer PRs.

K. Dve remains expressed in outer PRs upon deletion of *outer enh*. Dashed white circles indicate outer PRs.

L, N. Expression of downstream Dve targets (Rh3, Rh5, and Rh6) is unaffected in *outer enh* deletion mutants in 1 week old adults. Dashed white circles indicate outer PRs.

M, O. Variable derepression of Rh5 and Rh6 in outer PRs is observed in *outer enh* deletion mutants in 4 week old adults. Expression of Rh3 is unaffected in *outer enh* deletion mutants in 4 week old adults. Dashed white circles indicate outer PRs.

P. Knocking out Otd/Dve K50 binding sites resulted in an increased level of GFP in **y**R7s, suggesting that these sites mediate repression by Dve but not activation by Otd in **y**R7s. Solid yellow circles indicate **y**R7s that express GFP; solid white circles indicate **p**R7s that do not express GFP; dashed white circles indicate outer PRs and R8s. BS KO: binding site knockout.

Q. Binding of Dve is dependent on K50 Otd/Dve sites in ***y****R7 enh.* WT, wild type sequence; M, mutation of K50 Otd/Dve site. Arrows indicate the bands shifted upon Dve binding. Note, multiple bands are observed likely due to the presence of multiple functional DNA binding domains within Dve (Johnston et al., 2011), yielding higher-order DNA/protein structures.

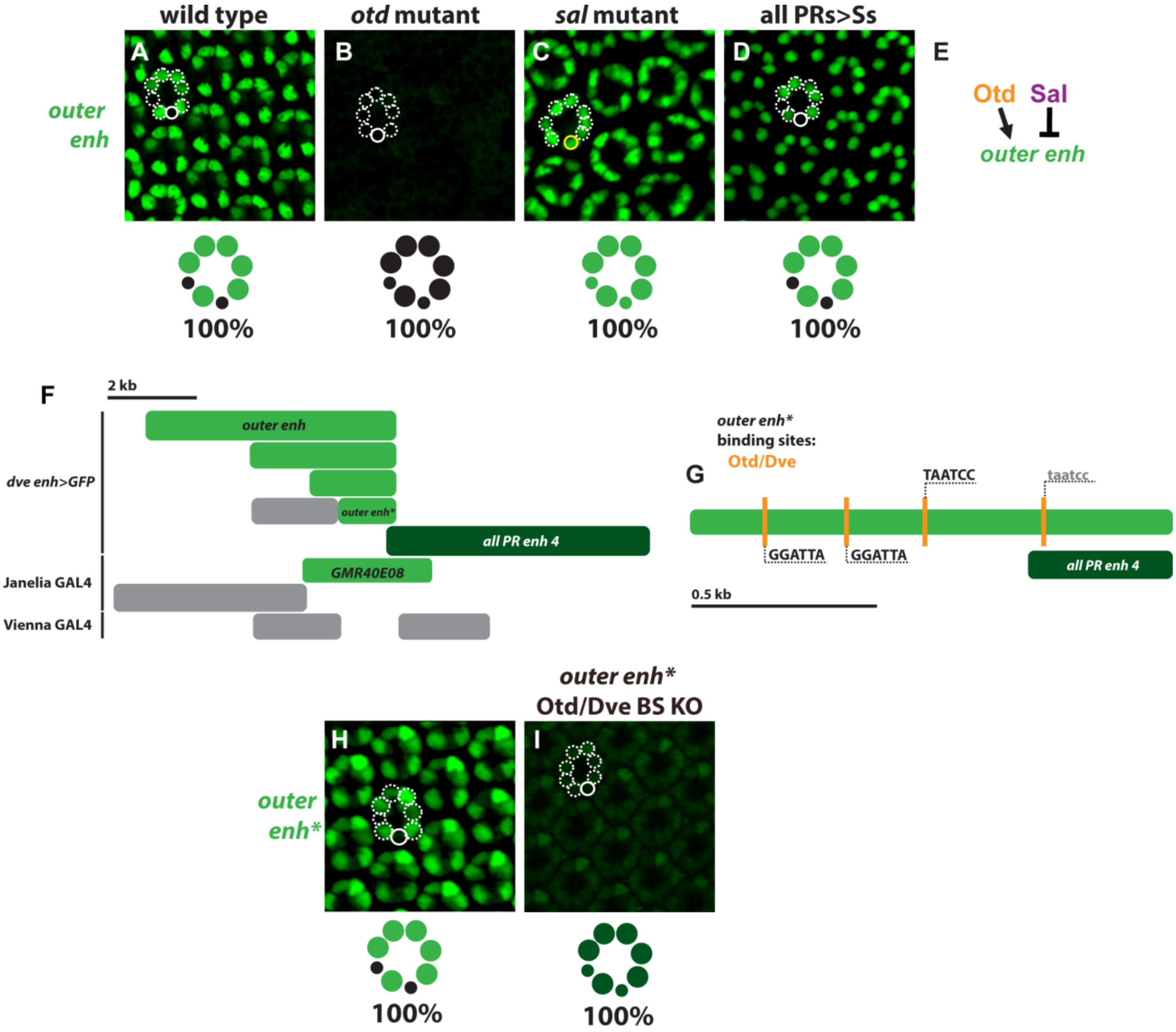

Figure 5. ***outer enh*** **is regulated by Otd and Sal**

For A-D and H-I, dashed white circles indicate outer PRs and R8s; solid white circles indicate **p**R7s; solid yellow circles indicate presumptive R7s expressing GFP. In schematics, light green circles indicate strong GFP expression, dark green circles indicate weak GFP expression, and black circles indicate no GFP expression. Expression analysis was conducted on mid-pupal retinas.

A. *outer enh* is expressed in outer PRs.

B. Expression of *outer enh* is lost in *otd* mutants.

C. *outer enh* is expressed in all PRs in *sal* mutants.

D. Expression of *outer enh* is unaffected by ectopic expression of Ss in all PRs.

E. Otd activates *outer enh* and Sal represses *outer enh.*

F. A truncated 1.3 kb fragment of *outer enh,* denoted *outer enh**, was sufficient to recapitulate GFP expression in outer PRs. Larger fragments encompassing *outer enh** also expressed GFP in outer PRs, as did Janelia reporter GMR40E04. Light green fragments drove strong GFP expression, dark green fragments drove weak GFP expression, and gray fragments did not drive GFP expression.

G. *outer enh** contains three conserved Otd/Dve binding sites. Capitalized black text indicates perfect conservation across 6 *Drosophila* species. Lower case gray text indicates that more than one species shows variation at the site.

H. *outer enh** is expressed in outer PRs, similar to Dve and *outer enh.*

I. Mutating Otd/Dve binding sites in *outer enh** resulted in a loss of expression of GFP. BS KO: binding site knockout. (Note, yellow circle indicates presumptive **y**R7)

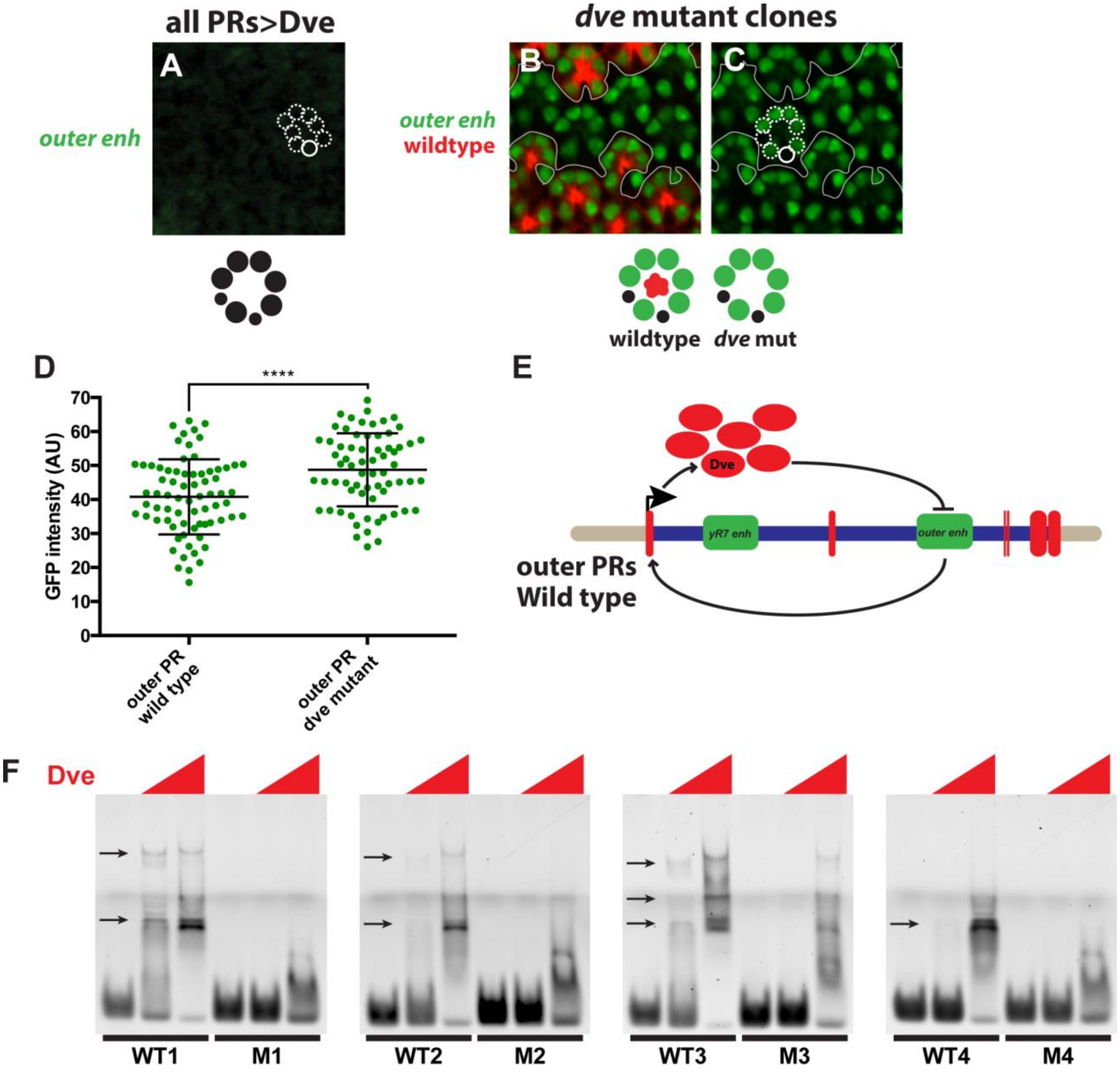

Figure 6. Dve feeds back to control *outer enh*

For A-C, dashed white circles indicate outer PRs and R8s; solid white circles indicate R7s. Expression analysis was conducted on mid-pupal retinas. In schematics, green circles indicate GFP expression, black circles indicate no GFP expression, and red spots indicate RFP expression.

For B-C, solid gray line represents boundary between *dve* mutant clones (indicated by absence of RFP) and wild type clones (indicated by presence of RFP).

A. Expression of *outer enh* is lost when Dve is ectopically expressed in all PRs.

B-C. Autoregulatory feedback: In outer PRs, *outer enh* is upregulated in *dve* mutant clones compared to wild type clones.

D. Quantification of outer PR GFP expression of *outer enh* in *dve* mutant clones compared to wild type clones. n=72 for wild type outer PRs and n=67 for *dve* mutant outer PRs. **** indicates p <0.0001, unpaired t test with Welch's correction. All measurements were internally controlled within a single mid-pupal retina.

E. *outer enh* induces Dve expression that negatively feeds back onto *outer enh* to maintain homeostatic levels in outer PRs.

F. Binding of Dve is dependent on K50 Otd/Dve sites in *outer enh.* WT, wild type sequence; M, mutation of K50 Otd/Dve site. Arrows indicate the bands shifted upon Dve binding. Note, multiple bands are observed likely due to the presence of multiple functional DNA binding domains within Dve (Johnston et al., 2011), yielding higher-order DNA/protein structures.

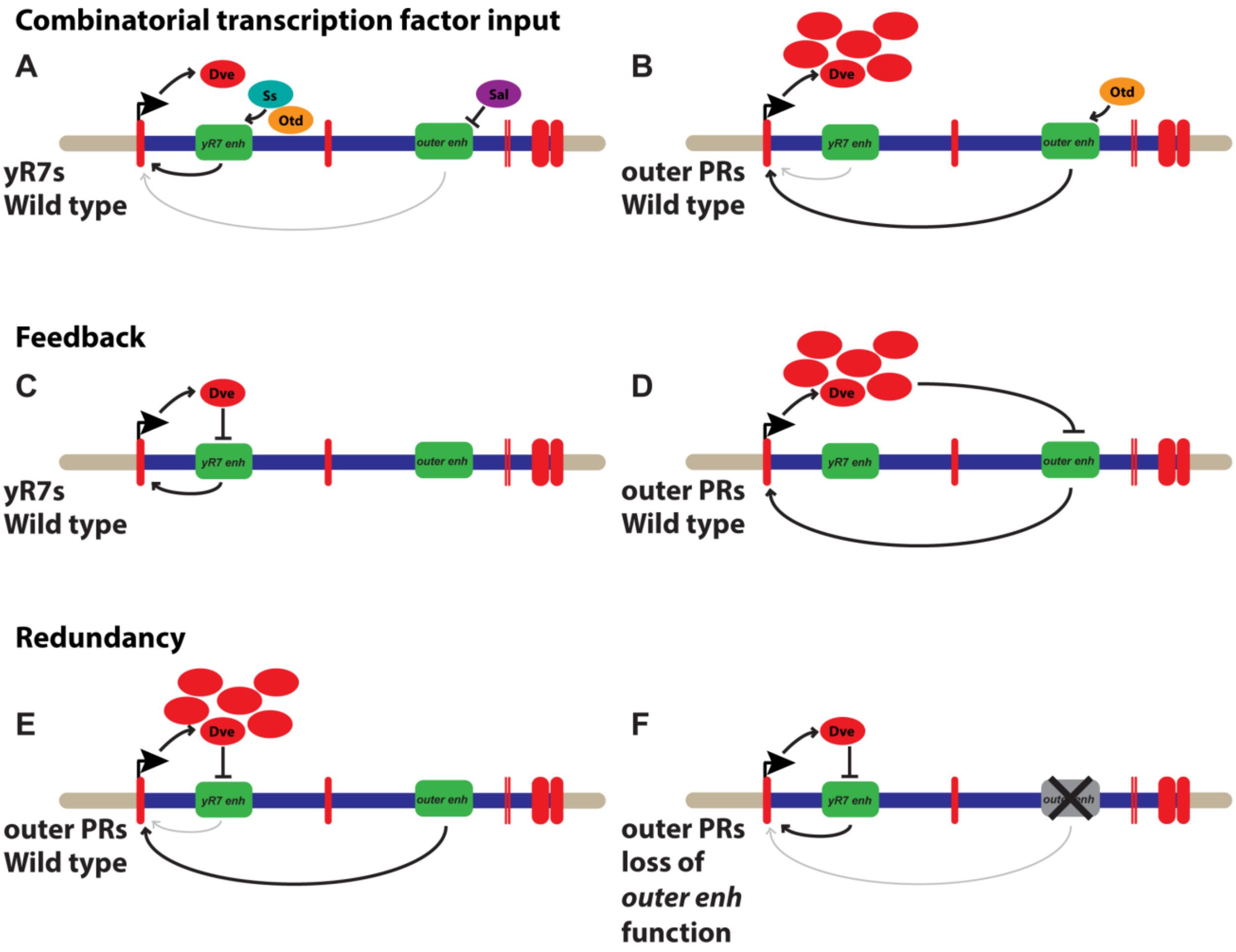

Figure 7. Combinatorial transcription factor input, feedback, and redundancy govern *dve* expression

A. In **y**R7 cells, ***y**R7 enh* is activated by Otd and Ss, while *outer enh* is repressed by Sal.

B. In outer PRs, Otd activates *outer enh*.

C. In **y**R7 cells, ***y**R7 enh* induces Dve expression that negatively feeds back onto ***y**R7 enh* to maintain homeostatic levels.

D. In outer PRs, *outer enh* induces Dve expression that negatively feeds back onto *outer enh* to maintain homeostatic levels.

E. In wild type outer PRs, *outer enh* induces Dve expression that negatively feeds back onto ***y****R7 enh* to completely repress expression.

F. Upon loss of *outer enh* function, ***y****R7 enh* is derepressed and drives expression in outer PRs.

Supplemental Figures

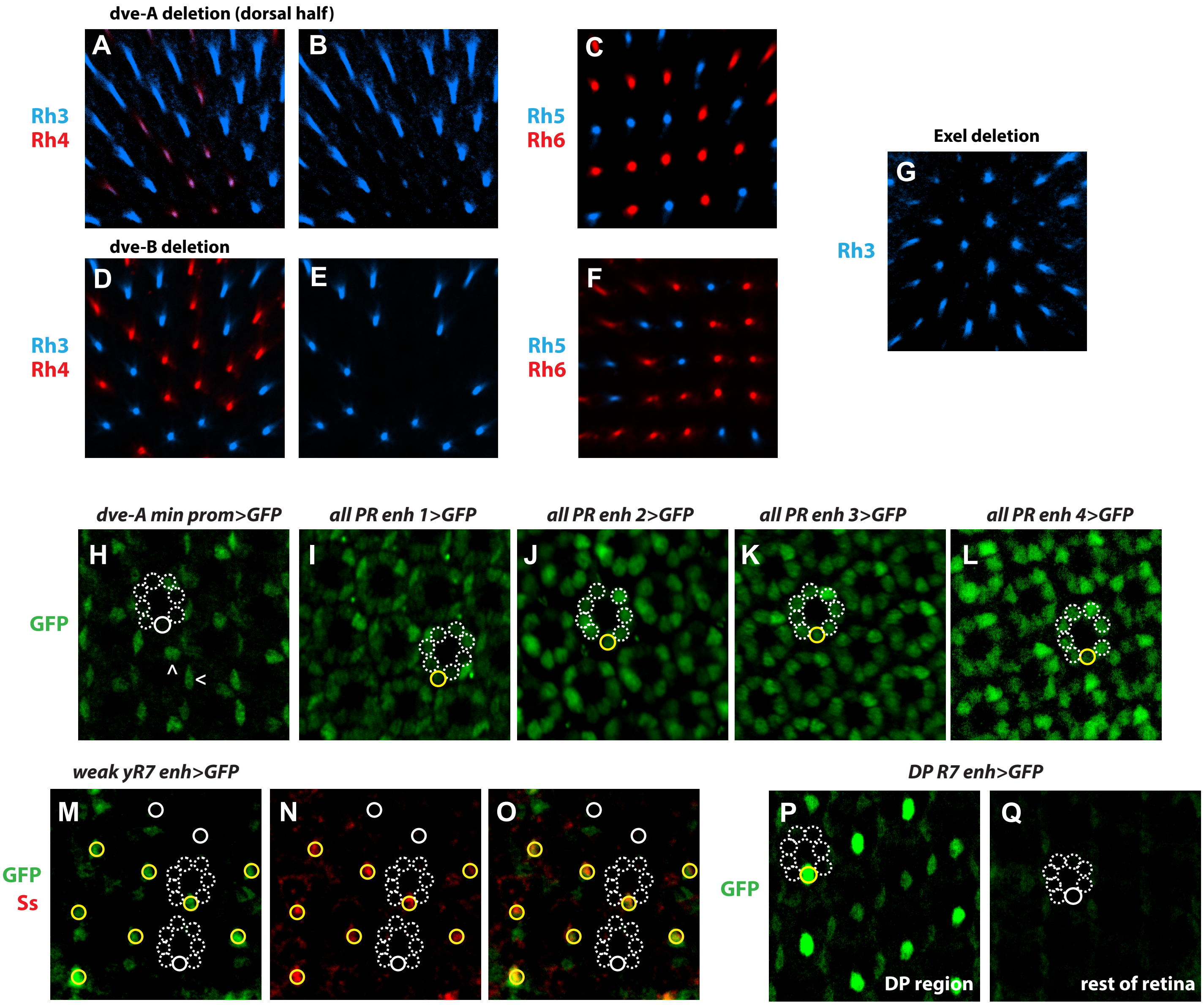

Figure S1. ***dve enh>GFP* constructs and *dve-A* and *dve-B* promoter deletions**

A-C. *dve-A* promoter deletion resulted in upregulation of Rh3 in all R7s in the dorsal half of the retina. Dve targets Rh5 and Rh6 displayed wild type expression.

D-F. *dve-B* promoter deletion displayed wild type expression of Dve targets (Rh3, Rh5, and Rh6).

G. *dve*^{exel} deletion, covering ***y****R7 enh* and the *dve-A* promoter, resulted in Rh3 upregulation in R7s.

H. *dve-A min prom* drove weak expression in R4s (denoted by ^) and pigment cells (denoted by <). Dashed white circles represent outer PRs and R8s; solid white circle indicates R7.

I-L. Four enhancers (*all PR enh 1-4*) drove weak GFP expression in all PRs. Dashed white circles represent PRs. Yellow circles denote GFP-expressing R7s.

M-O. *weak* ***y****R7 enh* displayed weak GFP expression in **y**R7s; Ss is a marker for **y**R7s. Dashed white circles represent outer PRs and R8s, solid white circles denote **p**R7s, and solid yellow circles denote **y**R7s.

P-Q. *dorsal R7 enh* drove expression in R7s in the dorsal posterior (DP) region of the retina. Dashed white circles represent PRs. Yellow circles indicate GFP-expressing R7; solid white circle indicates non-expressing R7.

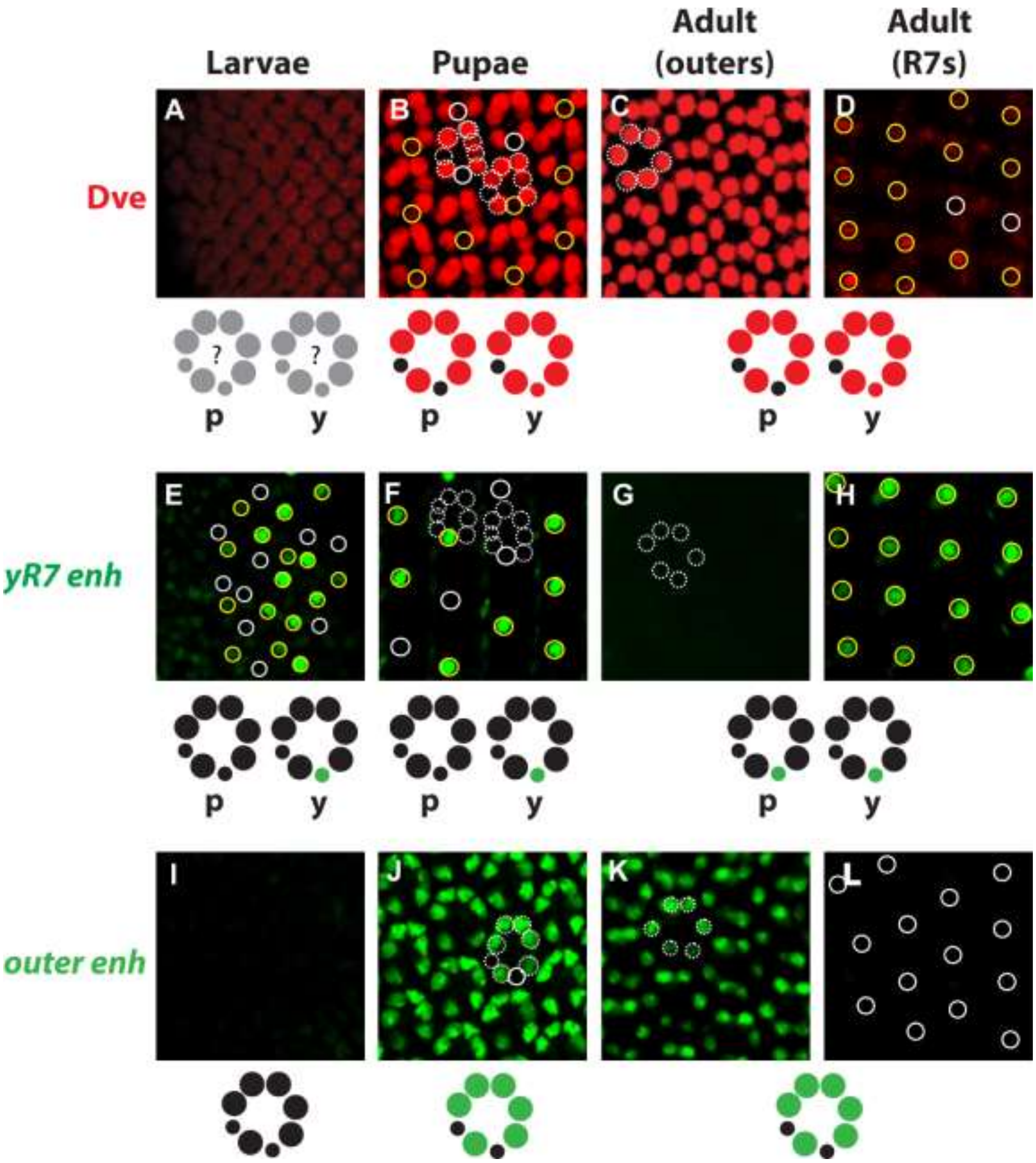

Figure S2. **Differential expression of Dve throughout development**

For A-L, in schematics, red circles indicate endogenous Dve expression, green circles indicate GFP expression, black circles indicate no expression (endogenous Dve or GFP), and gray circles indicate indeterminate expression.

For B-D, yellow circles indicate **y**R7 cells. Solid white circles indicate **p**R7 cells. Dashed white circles are outer PRs and R8s.

For E-H, yellow circles indicate **y**R7 cells. Solid white circles indicate **p**R7 cells. Dashed white circles are outer PRs and R8s.

For J-L, dashed white circles represent outer PRs; solid white circles indicate R7s.

A. Antibody staining for Dve is nonspecific in larvae.

B-D. Dve is highly expressed in outer PRs and weakly expressed in **y**R7s in pupae and adults.

E-F. ***y****R7 enh* is expressed in **y**R7s in larvae and pupae.

G-H. ***y****R7 enh* is expressed in all R7 cells in the adult but is not expressed in outer photoreceptors.

I. *outer enh* is not expressed in larvae.

J-L. *outer enh* drives expression in outer PRs in pupae and adults, but is not expressed in R7s.

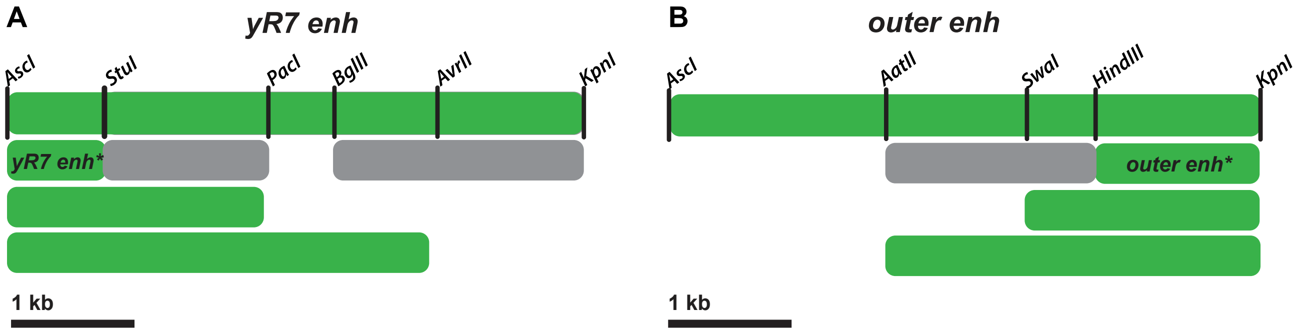

Figure S3. Restriction enzyme sites used to generate *dve enh* truncations

A. Schematic of the ***y****R7 enh* and the restriction enzyme sites used to generate the ***y****R7 enh** and other truncations.

B. Schematic of the outer enh and the restriction enzyme sites used to generate the *outer enh** and other truncations.

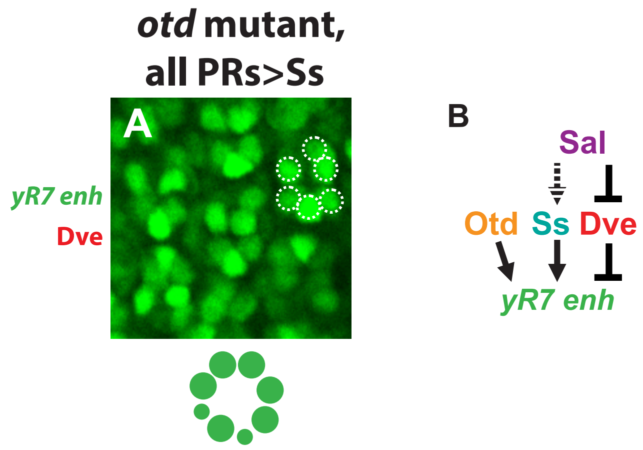

Figure S4. Sal activates yR7 enh by repressing Dve

A. In *otd* mutants, in which Dve is not expressed, ectopic Ss induces ***y****R7 enh* in all PRs.

B. The regulatory interactions governing ***y****R7 enh.* Otd and Ss activate ***y****R7 enh*, while Dve represses ***y****R7 enh*. Sal activates stochastic expression of Ss (denoted by dashed arrow) in **y**R7s and represses Dve.

Supplementary Materials and Methods

Generating *dve enh>GFP* constructs

3-6kb fragments (Fig. 2A) were amplified using DNA isolated from yw^{67} flies and ligated into the pGEM-T easy vector. The 699 bp *dve* minimal promoter was subcloned into a pJR16 nGFPcDNA reporter vector containing a w^+ marker, generating the pGG14 vector. Other fragments of the *dve* locus were subcloned into pGG14 before microinjection into fly embryos. Constructs were then integrated into the genome via the attP/B system, and injected flies were crossed with a balancer stock with the genotype y^-w^-*; +/+; Tm2/Tm6b*. Red-eyed offspring were isolated, and transgenes were balanced over Tm6b. Primers and restriction enzymes used to generate each *dve* enhancer construct are shown in Table S1.

Enhancer constructs ***y***_R7 enh>GFP_ and *outer enh>GFP* were further truncated using restriction enzymes and blunt end ligation (Fig. S3A,B). Reporter vectors were microinjected into fly embryos, and transgenic lines were established using the same methods as above.

Drosophila strains

Flies were raised on standard cornmeal medium and grown at room temperature (25°C). Transgenic lines used include *dve* enhancer gene constructs generated for this project, as well as the reagents in Table S2.

The GAL4-UAS system was used to ectopically express Sal, Ss, and Dve (Brand and Perrimon, 1993), while the FLP-FRT system was used to create *sal* and *dve* mutant phenotypes (O'Gorman et al., 1991). Shortened and complete genotypes of flies examined are found in Table S3.

Janelia and VDRC Stock Centers generated transgenic lines that express GAL4 driven by flanking non-coding or intronic regions of various genes. GAL4 lines associated with *dve* ***y****R7* and *dve outer* enhancer elements were crossed with UAS-nlsGFP. See Table S4.

CRISPR-generated deletions

dve-B promoter, *outer enh*, and ***y****R7 enh* deletions were generated using CRISPR. We designed four gRNAs per deletion, two flanking either side of the deletion. Forward and reverse strands of gRNAs were designed and annealed together to have BbsI restriction site overhangs. gRNAs were then cloned into the pCDF3 cloning vector. Single stranded homologous bridges were generated with 80 bp homologous regions flanking each side of the deletion. An AscI restriction cut site was incorporated into the homologous bridge to facilitate screening. For every deletion, all four gRNAs were injected into *Drosophila* embryos at 125ng/ul each for a total of 500ng, along with 100ng/ul of homologous bridge oligos. Single adult males were then crossed with balancer stocks (yw ; if / cyo ; +), and the progeny were screened for the deletion via PCR. Homologous bridges, gRNAs, and PCR screening primers are shown in Table S5.

Otd/Dve binding site knockout

Otd/Dve binding site knockouts for *outer enh* and ***y****R7 enh* were generated using site-directed mutagenesis, where the K50 homeodomain consensus sites (TAATCC) were replaced with AAAAAA. Constructs were integrated into the genome and *Drosophila* strains were established using the same methods as described above.

Electrophoretic Mobility Shift Assay

Binding assays were performed as previously described (Johnston et al., 2011; Li-Kroeger et al., 2008).

Probes tested were as follows (bold/underline indicates K50 Otd/Dve site or mutated K50 Otd/Dve site):

y*R7 enh* 1 5’ –CGTGTTAGCCAAACC**TAATCC**AGGCTAAACGAGGG- 3’
y*R7 enh* 2 5’ –AAATACGCTTATGTC**GGATTA**TCCCATAATTTATG- 3’
y*R7 enh* mutant 1 5’ –CGTGTTAGCCAAACC**TGCGCC**AGGCTAAACGAGGG- 3’
y*R7 enh* mutant 2 5’ –AAATACGCTTATGTC**GGCGCA**TCCCATAATTTATG- 3’
outer enh 1 5’ –AGCAAACAACAAAAA**GGATTA**AGTCCAAGACACAC- 3’
outer enh 2 5’ –ATACTTATTTCATTA**GGATTA**TTTTTGACTAACAT - 3’
outer enh 3 5’ –TCACGGCATTAATTA**TAATCC**GCTTAAAAGTTTCA - 3’
outer enh 4 5’ –TCACACAAGGATTCG**TAATCC**TTGCGAGGGACCCA- 3’
outer enh mutant 1 5’ –AGCAAACAACAAAAA**GGCGCA**AGTCCAAGACACAC- 3’
outer enh mutant 2 5’ –ATACTTATTTCATTA**GGCGCA**TTTTTGACTAACAT- 3’
outer enh mutant 3 5’ –TCACGGCATTAATTA**TGCGCC**GCTTAAAAGTTTCA- 3’
outer enh mutant 4 5’ –TCACACAAGGATTCG**TGCGCC**TTGCGAGGGACCCA- 3’

Antibodies

Antibodies and dilutions used were as follows: mouse anti-prospero (1:10)(DSHB), rat anti-Elav (1:50)(DSHB), sheep anti-GFP (1:500), mouse anti-Rh3 (1:100)(gift from S. Britt, University of Colorado), rabbit anti-Rh4 (1:100)(gift from C. Zuker, Columbia University), mouse anti-Rh5 (1:2000)(Tahayato et al., 2003), rabbit anti-Rh6 (1:2000)(Tahayato et al., 2003), guinea pig anti-Ss (1:200)(Gift from Y.N. Jan, University of California, San Francisco), rabbit anti-Dve (1:500)(Nakagoshi et al., 1998). All secondary antibodies were Alexa-conjugated (1:400) (Molecular Probes).

Retina dissection and immunohistochemistry

Retinas were dissected and stained as described previously (Hsiao et al., 2012). Larvae were collected and dissected in ice cold PBS (1x), and retinas were isolated using forceps before fixing for 20 minutes in 4% formaldehyde at RT. Samples were washed three times with PBX and kept in primary antibodies diluted in PBX overnight at 4°C. After three washes with PBX, secondary antibodies diluted in PBX were added, and samples were kept at RT for at least 2 hours. After three more washes, samples were kept in PBX at room temperature overnight, before being mounted flat in Vectashield (Vector Laboratories).

To facilitate pupae collection at the desired mid-pupae stage, flies were raised at 25ºC in a 12hr light/12hr dark cycle incubator. Pupae heads were dissected in ice cold PBS (1x) and eye-brain complexes were extracted via pipetting. Fixing, antibody staining and mounting procedures were consistent with those of larvae, but pupal retinas were not isolated from the brain until prior to mounting.

Adult flies were anesthetized on CO_2 pads before their heads were removed using forceps. Fly heads were dissected in ice cold PBS (1x), and retinas were isolated using forceps. Fixing and antibody staining procedures were consistent with those of larvae and pupae, although laminas were not removed until after fixing. Retinas were then mounted using SlowFade Gold Reagent (ThermoFisher Scientific).

For all stages of fly development, samples stained with antibodies were visualized under a Zeiss LSM 700 confocal microscope.

Quantification

Fluorescence intensity of nuclear GFP expression of single retinas was quantified using the ImageJ processing program. A small region in the center of each nucleus was selected for fluorescence intensity measurement. Images were taken under subsaturating conditions and comparisons of GFP intensity were drawn between cells of the same retina. Column scatterplots were generated using Graphpad Prism.

Table S1. *dve enh>GFP* Constructs and Primers

Construct	**Primers**	**Restriction sites**
***y**R7 enh*	agtcggcgcgcccacaaccatttcactcctgc agtcggtacccttctcccagtcttcgaatg	*AscI* *KpnI*
outer enh	agtcggcgcgcctcatcctcatccctacctac agtcggtaccacaactgcctttgccttgtg	*AscI* *KpnI*
***y**R7 enh extended to right*	agtcggcgcgccgcctagctaccgtgatcaac agtcggtaccgtttagctcgattacgcttc	*AscI* *KpnI*
dve min promotor	agtcagatcttgatctggctctctggactc agtcggatccgtgggaaagtgttggtaagc	*BglII* *BamHI*
*weak **y**R7 enh*	agtcggcgcgcccggtcagcaggtgagttgag agtcggtacctacgatgacaccgataagcg	*AscI* *KpnI*
dorsal R7 enh	agtcggcgcgcccataatcacaacacgagtcgg agtcggtaccgatggtggcttaactcaatc	*AscI* *KpnI*
all PR enh 1	agtcggcgcgccgcttatctgcggctttgtgg agtcggtaccctcgtcttgtcccgattcca	*AscI* *KpnI*
all PR enh 2	agtcggcgcgccgctagcgcatagagcatagatg agtcggtaccgttgctggcaccaatacacg	*AscI* *KpnI*
all PR enh 3	agtcggcgcgccgtgctgcctacaagtttgga agtcggtaccgccttctgaagactagcac	*AscI* *KpnI*
all PR enh 4	agtcggcgcgcccgaaactcctcgactcacac agtcggtaccccaattcgctgattg	*AscI* *KpnI*
dve enh 1	agtcggcgcgcccactgacatcaattcaccgtc agtcggtaccaggagaaaggagtgagttcg	*AscI* *KpnI*
dve enh 2	agtcggcgcgccccatcccttagagagctttg agtcggtacctgtatctggggaatcggatg	*AscI* *KpnI*
dve enh 3	agtcggcgcgccgccacaatgtcaagcatcaaag agtcggtacccactttcccacagtatcatcttg	*AscI* *KpnI*
dve enh 4	agtcggcgcgcccagagctgaactgaacaatc agtcggtacccgtgtctctgcgctttgtga	*AscI* *KpnI*
dve enh 5	agtcggcgcgccgtcttagtgcagctactgtt agtcggtaccgaaggcttacgaaactaatg	*AscI* *KpnI*
dve enh 6	agtcggcgcgcccagctcgttaagcataagca agtcggtacccgttcccaaattaccccatc	*AscI* *KpnI*
dve enh 7	agtcggcgcgcctggtggtggcgattcatttg agtcggtaccctaccacaaaactagagcaccc	*AscI* *KpnI*

Table S2. ***Drosophila*** **reagent descriptions**

Name	**Description**	**Source**
otd^{uvi}	hypomorphic allele, fails to produce protein product in the eye	(Vandendries et al., 1996)
FRT40 sal$^{Df(2L)32FP5}$	a deficiency that removes the *sal* gene	(Barrio et al., 1999)
FRT42d dve^{186}	Dve protein null mutant	(Terriente et al., 2008)
FRT40 GMR-hid, cL	eye-specific enhancer driving hid, an activator of apoptosis	Bloomington
FRT42d GMR-RFP	eye-specific enhancer driving RFP	Bloomington
ey-FLP	eye-specific enhancer driving flippase	Bloomington
ss$^{d115.7}$	Ss protein null mutant	(Duncan et al., 1998)
ss$^{Df(3R)Exel7330}$	Deficiency covering the *ss* locus	Bloomington
UAS-Sal	UAS enhancer driving Sal	(Kuhnlein and Schuh, 1996), (Wernet et al., 2003)
UAS-Dve	UAS enhancer driving Dve	(Nakagoshi et al., 1998)
UAS-Ss	UAS enhancer driving Ss	(Duncan et al., 1998)
lGMR-Gal4	eye-specific enhancer driving Gal4	Bloomington
dve^{Exel}	deletion that removes the first exon of *dve, dve-A* promoter, and *dve* ***y****R7* enhancer element	See footnote*
dve^{E181}	deletion allele for the *dve-A* promoter	(Nakagawa et al., 2011)
UAS-nlsGFP	UAS driving nuclear GFP	Bloomington

*We generated the dve^{exel} deletion by using hsFLP-mediated recombination between two FRT sites, inserted by P-elements P(XP)d05100 and P(XP)d08355.

Table S3. *Drosophila* shortened and complete genotypes

Shortened	**Complete genotype**	**Figure**
dve enh>GFP	*yw ; + ; dve enh>GFP*	2B-E, 3A, 5A, S1H-Q, S2E-L
all PRs>Ss	*yw ; lGMR>Gal4, UAS>Ss ; dve enh>GFP*	3E, 5D
all PRs>Sal	*yw, UAS>sal ; lGMR>Gal4 ; dve enh>GFP*	3G
all PRs>Dve	*yw ; lGMR>Gal4 ; dve enh>GFP/ UAS>dve*	4A, 6A
sal mutant	*yw ;*$sal^{Df(2L)32FP5}$*FRT40 GMR>hid FRT40 ; dve enh>GFP/ey>Flp*	3F, 5C
otd mutant	otd^{uvi} *; + ; dve enh>GFP*	3B, 5B
dve mutant	*ey>FLP ;FRT42d* dve^{186}*/ FRT42d GMR>RFP ; dve enh>GFP/ +*	4B-E, 6B-C
ss mutant	*yw ; + ; dve enh>GFP,* $ss^{BL7985def}$*/* $ss^{d115.7}$	3C
all PRs>Ss and Sal	*yw, UAS>sal ; lGMR>GAL4, UAS>ss ; dve enh>GFP*	3H
otd mutant, all PRs>Ss	otd^{uvi} *; lGMR>GAL4, UAS>ss ; dve enh>GFP*	S4A
dve-A del	*yw ; FRT42d* dve^{186} / dve^{E181} *; +*	S1A-C

Table S4. Janelia and VDRC Gal4 stock numbers

Janelia GMR			
49373	49927	48655	46230
45702	50133	45682	46238
45284	46241	50066	48150
41238			
VDRC Stock			
020724	020725	020737	020739

Table S5. Primers for CRISPR

dve-B del	
Homologous bridge	ttttatggatcgcttggcattataatgaacagcggcgtcgccggctggccatgggcgcatggcgcgcccatgggagcaagttggagctgggcaagcccccacatcccatccgcccactgacctaagcc
dveBgRNA1 F	gtcgctggccatgggcgcataat
dveBgRNA1 R	aaacattatgcgcccatggccagc
dveBgRNA2 F	gtcgggataagtacggtgcatgg
dveBgRNA2 R	aaacccatgcaccgtacttatccc
dveBgRNA3 F	gtcgtcatccttccagtgcccat
dveBgRNA3 R	aaacatgggcactggaaggatgac
dveBgRNA4 F	gtcggtgtctgccactgttgaac
dveBgRNA4 R	aaacgttcaacagtggcagacacc
DveBscr F	gctgttgggagattaagttt
DveBscr R	tgccttctgaagactagcac
outer enh del	
Homologous bridge	gctgcctgggcgtccttttctcgggcacttgatagaatttgacaaattgaaaatccttttggcgcgccgaagcctacttaagtcccttgaaatccttgagatttttttgcactggtcaagcaatgataa
outergRNA1 F	gtcggacaaccgctcgccacaaa
outergRNA1 R	aaactttgtggcgagcggttgtcc
outergRNA2 F	gtcgttcaagagtccaggcgacc
outergRNA2 R	aaacggtcgcctggactcttgaac
outergRNA3 F	gtcgaaattaagcaatagtctta
outergRNA3 R	aaactaagactattgcttaatttc
outergRNA4 F	gtcggacttaagtaggcttccca
outergRNA4 R	aaactgggaagcctacttaagtcc
outer-scr F	ccagtgattatgtatggttc
outer-scr R	gagtgatttgggtatttagg
yR7 enh del	
Homologous bridge	acttgctccccgtccgtcgatcgattcaaattaccagcgatttattggcgatcgccagccggcgcgccgctatggcaatgcaaacaggtgagggtgaattacttgtcctagacaactttgcagtcagc
yR7gRNA1 F	gtcgttgatcacggtagctaggc
yR7gRNA1 R	aaacgcctagctaccgtgatcaac
yR7gRNA2 F	gtcgtgttcgcataacgctggtc
yR7gRNA2 R	aaacgaccagcgttatgcgaacac
yR7gRNA3 F	gtcgtttagctcgattacgcttc
yR7gRNA3 R	aaacgaagcgtaatcgagctaaac
yR7gRNA4 F	gtcgtttgcattgccatagctac
yR7gRNA4 R	aaacgtagctatggcaatgcaaac
yR7-scr F	gatggctaatggcgagagga
yR7-scr R	gcaatcttggcactcccgtt